Cooperative Approaches in Catalytic Hydrogenation and Dehydrogenation

Michael A. Stevens[a] and Annie L. Colebatch*[a]

DOI: 10.1039/D1CS01171E

Metal-ligand cooperativity (MLC) is an established strategy for developing effective hydrogenation and dehydrogenation catalysts. Metal-metal cooperativity (MMC) in bimetallic complexes is not as well understood, and to date has had limited implementation in (de)hydrogenation. Herein we use (de)hydrogenation processes as a platform to examine modes of cooperativity, with a particular focus on catalytic mechanisms. We investigate how lessons learnt from the extensive development of metal-ligand cooperative catalysts can aid the ongoing development of metal-metal cooperative catalysts.

Key Learning Points:

1. Learn to identify different modes of cooperative reactivity and understand mechanistic signatures of cooperativity.
2. Appreciate the breadth of application of catalytic hydrogenation and dehydrogenation processes.
3. Recognise metal-ligand cooperativity as a tool for highly efficient catalytic (de)hydrogenation.
4. Recognise metal-metal cooperativity is an emerging strategy in catalytic (de)hydrogenation.
5. Appreciate similarities and differences between metal-ligand cooperativity and metal-metal cooperativity.

1. Introduction

The development of homogeneous transition metal catalysis has revolutionised chemical synthesis. Historically, most advances feature single-site catalysts, in which a transition metal is surrounded by carefully designed ligands to optimise the steric and electronic environment at the reactive metal centre, where all reactions take place. Cooperative catalysis, in which multiple sites in the catalyst participate in reactivity, is now an established alternative to single-site reactivity.[1–3] Inspiration from the complexity of enzymatic catalysis is commonly cited within the field.[1,3,4] Enzymes can be thought of as the ultimate cooperative systems, wherein cooperation of many chemical entities is required for the high efficiency and selectivity exhibited. This encompasses multimetallic active sites or cofactors as well as interactions with neighbouring ligands, protein scaffolds or the secondary coordination sphere.

Synthetic chemists have developed innovative approaches to incorporate cooperative effects into molecular systems.[5] Within transition metal catalysis, metal-ligand cooperativity (MLC)[1,2,6,7] and metal-metal cooperativity (MMC)[3] are two major strategies. Ongoing developments in this space are driven by the discovery of new chemical reactions, the unique reactivity and selectivity profiles that can emerge, the drive to utilise earth-abundant 3d metals that do not undergo simple two-electron redox processes, and scientific curiosity.

This review aims to provide readers with an overview of the concept of cooperativity in homogeneous organometallic catalysis, and outline examples of this using case studies from hydrogenation and dehydrogenation catalysis. (De)hydrogenation reactions are pervasive across chemistry, including in energy applications,[8,9] polymers,[10] fine chemical production and asymmetric synthesis.[11] (De)hydrogenation processes are considered green as they are one of the most atom economical transformations and typically have limited by-products. While the concept of metal-ligand cooperativity has been comprehensively studied and implemented in a broad array of catalytic processes, the field of metal-metal cooperativity is much less developed. We consider similarities and differences between these two approaches, and outline future directions and challenges in the field.

2. The Concept of Cooperativity in Catalysis

The term cooperativity (and related terms such as synergism) is used to describe the enhanced effects obtained from the combination of multiple chemical entities.[12] This applies to a wide array of scenarios in the chemical literature.[12,13] For the purposes of this review, we will focus on a subset of cooperativity relevant to homogeneous catalysis.

Traditional organometallic catalysts operate via single-site, non-cooperative mechanisms in which reactivity occurs exclusively at the metal centre (Figure 1(a)). An alternative to this, referred to as multisite, bifunctional or cooperative reactivity, exists where multiple sites within a catalyst participate in reactivity (Figure 1(b), 1(c)). This has been defined as sites that undergo reversible bond formation/cleavage and are chemically modified in the process.[6] This is classified according to the nature of the two reactive sites as either metal-ligand cooperativity (MLC)[6] or metal-metal cooperativity (MMC, also referred to as bimetallic cooperativity).[3] Within these categories, cooperativity can take on a variety of forms, as demonstrated for H_2 activation in Figure 1. MLC is typically classified into metal-Lewis base reactivity, metal-Lewis acid reactivity or aromatisation-dearomatisation reactivity.[1] For MMC, however, there is no universal classification scheme. The variety of reactivity processes that can occur are covered in section 4.

[a.] Research School of Chemistry, Australian National University, Canberra, ACT 2601, Australia. Email: annie.colebatch@anu.edu.au.

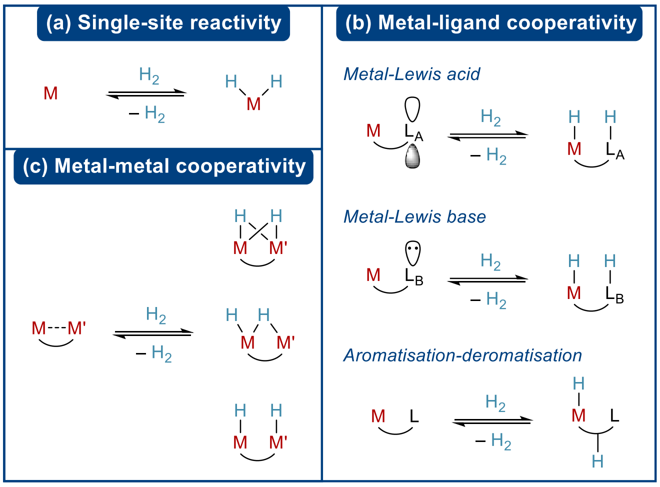

Figure 1. (a) Single-site and multisite ((b) MLC, (c) MMC) approaches to H_2 activation.

Scope

This work will survey examples of hydrogenation and dehydrogenation processes catalysed by transition metal complexes in which mechanistic evidence reveals bifunctional metal-ligand or metal-metal cooperativity plays a part of the catalytic cycle. Other forms of cooperativity will be excluded, such as redox active ligands or metal-metal cooperativity in which the second metal acts in a supporting electronic role. The examples of MMC are limited to molecular bimetallic systems, and exclude higher nuclearity complexes and clusters. Related concepts in which two separate catalysts partake, such as dual catalysis and tandem catalysis, will not be included.

3. Metal-Ligand Cooperativity

The field of metal-ligand cooperativity is well-established and has been the subject of extensive reviews.[1,2,6] The aims of the coverage here are to present an overview of key features of MLC, illustrated with characteristic examples, and provide the context to frame MMC. MLC reactivity and so-called non-innocent ligands fall into a range of classes, with redox-active ligands,[14] structurally-responsive ligands[15] and bifunctional systems[1,2,6] being the most common. The latter is the focus of this work, wherein bifunctional or multisite reactivity across the metal and ligand occur on-cycle. Within this, the vast majority of systems involve ligands that feature a Lewis basic moiety, with ligands that undergo reversible aromatisation-dearomatisation reactions a large subset of this. MLC via ligands that feature a Lewis acid moiety is still an emerging area of (de)hydrogenation catalysis.[16]

The importance of MLC pathways in stoichiometric (de)hydrogenation studies has been demonstrated frequently,[17–21] but this can be difficult to translate to catalytic regimes which are extremely challenging to study experimentally. Much of the mechanistic information relies instead on computational studies. Some systems capable of MLC have been proposed to operate via non-cooperative single-site[22,23] or outer-sphere[24–27] pathways during catalysis. This tutorial review focuses on the conventional mechanisms proposed, but it is important to recognise that this is an ongoing area of study in the literature.

Metal-Lewis Base Cooperativity

Cooperative (de)hydrogenation catalysis featuring a ligand acting as a Lewis base is widespread. The ligand acts in a proton-responsive capacity. H_2 activation or substrate dehydrogenation proceed via heterolytic cleavage, with hydride transfer to the metal and proton transfer to the Lewis basic moiety either in a stepwise or concerted manner (Figure 2). The presence of hydridic and protic hydrogens facilitates low energy H_2 transfer to a polarised substrate (e.g. ketone), through hydride transfer to the $\delta+$ site (e.g. C) and proton transfer to the $\delta-$ site (e.g. O) (Figure 2). This pairing means efficient catalysis is encountered with polar substrates, predominantly CO and CN moieties. Amines feature most commonly as the Lewis basic site, but numerous other examples exist, particularly oxygen- and carbon-based Lewis bases. One notable distinction from traditional single-site catalysis is that metal-Lewis base cooperativity typically involves no change in the metal oxidation state during catalysis. The redox inactive role of the metal has enabled development of a wide variety of catalysts featuring earth abundant 3d transition metals.[1,7]

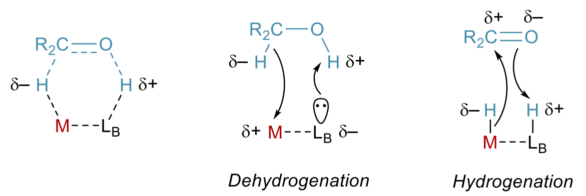

Figure 2. Proton and hydride transfer processes are common to metal-Lewis base and aromatisation-dearomatisation mechanisms for (de)hydrogenation of polar substrates.

Pioneering work was undertaken by the Noyori group, whose findings inspired significant growth in the field. Noyori-type catalysts for asymmetric hydrogenation feature a metal centre coordinated to a Lewis basic amide moiety. The conventional mechanism of asymmetric ketone hydrogenation with archetypal Ru catalyst [Ru{NTs(CHPh)$_2$NH}(mesitylene)] (**1**) is shown in Scheme 1.[28,29] This proceeds either via direct hydrogenation with H_2 or transfer hydrogenation in which in situ dehydrogenation of ^{i}PrOH is the source of hydrogen. This species can facilitate the heterolytic cleavage of H_2 or the dehydrogenation of ^{i}PrOH across the Ru-amide bond to generate the amino ruthenium hydride species **1a**. The subsequent substrate hydrogenation occurs via proton (N–H) and hydride (Ru–H) transfer. This process occurs with high enantioselectivity, with enantiomeric excesses often >90%. A revised mechanism has been proposed on the basis of computational studies that proceeds via an outer-sphere process.[24] In this case the amine N–H bond remains intact but interacts with the substrate via hydrogen-bonding.

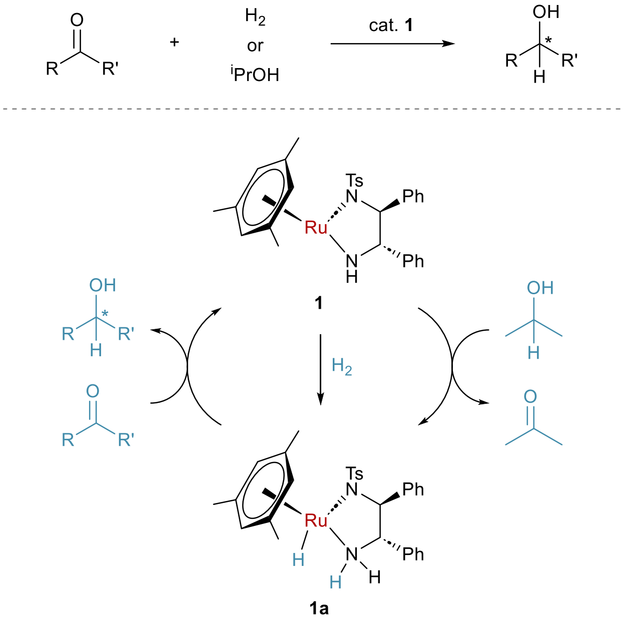

Scheme 1. Proposed mechanism of asymmetric hydrogenation and transfer hydrogenation of ketones catalysed by a Noyori-type ruthenium catalyst.[28,29]

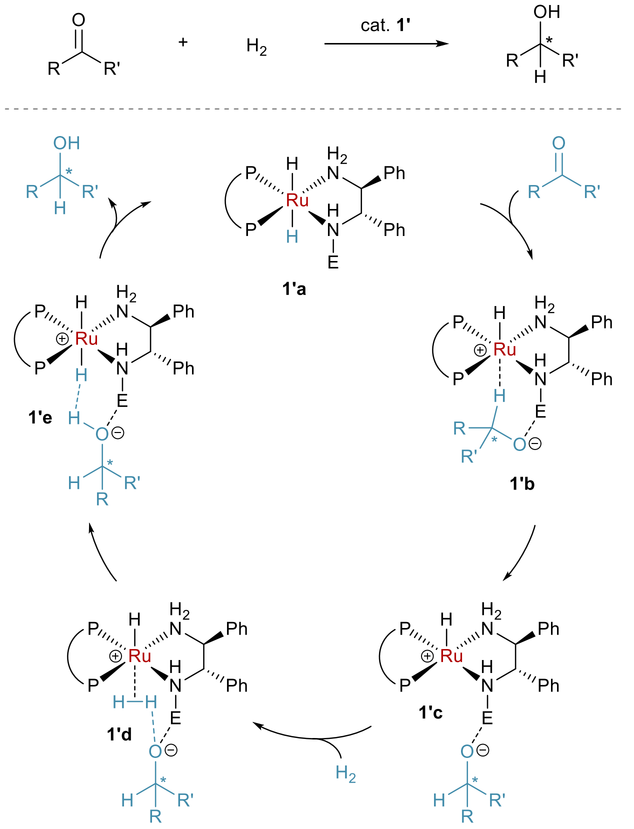

Scheme 2. Simplified proposed outer-sphere mechanism of asymmetric hydrogenation of ketones catalysed by a Noyori-type ruthenium catalyst. In the absence of base E = H, in the presence of KO^{t}Bu E = K or H; P^P = BINAP.[25]

It is important to point out that for numerous metal-Lewis base catalysts, including aromatisation-dearomatisation catalysts, alternative outer-sphere mechanisms have been proposed in which the ligand does not undergo bond formation or cleavage processes.[24,26,27,30] In these cases the Lewis base–H bond (or Lewis base–K bond in the presence of KO^{t}Bu base) remains intact throughout catalysis. Non-covalent interactions between the ligand and substrate are responsible for the high catalytic activity. The role of the Lewis base is multifaceted: (i) substrate activation through (Lewis base)–H···O hydrogen bonding (or (Lewis base)–K···O ionic interactions) which polarises the C=O bond to facilitate M–H to C hydride transfer, (ii) transition state stabilisation of rate-determining steps, (iii) substrate orientation for the enantio-determining hydride transfer, and (iv) substrate positioning to support M–H···H–substrate dihydrogen bonds.[30]

An example of this is depicted for Noyori-type catalysts in Scheme 2 below. Depending on the reaction conditions, the N,N ligand can be present as either the amine (E = H) or deprotonated in the presence of KO^{t}Bu to form a potassium amide (E = K). The N–E linkage is retained throughout catalysis and is involved in crucial non-covalent interactions with the substrate. N–E···O interactions activate the ketone substrate towards hydride transfer from Ru–H to form an alkoxide. Protonation of the alkoxide proceeds via a Ru(H_2) complex, again facilitated by non-covalent interactions between the alkoxide and N–E ligand as well as between the alkoxide and dihydrogen ligand. Related outer-sphere mechanisms have been proposed for other metal-Lewis base catalysts such as PNP pincer catalysts[26] and Milstein-type PNN pincer catalysts.[27] These will not be discussed in detail here, but readers are encouraged to refer to detailed accounts of the topic for more information.[24,30,31]

MLC reactivity across an M–N linkage has been extended using pincer ligands, particularly with widely applied PNP systems $NH(CH_2CH_2PR_2)_2$. In an illustrative example, Jones and co-workers reported the dehydrogenation of *N*-heterocycles with the iron PNP precatalyst [FeH(BH_4)(CO)(PNP)] (**2**).[17] The proposed mechanism is shown in Scheme 3, where cycling between metal-bound amido and amine states enables catalytic turnover. Independent synthesis of and catalytic testing with the amido complex **2a** confirmed it is an active species. Replacement of the N–H group of **2b** with N–Me completely supressed catalytic turnover, supporting the essential role of the cooperative N–H moiety for activity.[32] DFT studies suggest that the polarity of the substrate affects the mechanism. Polarised C–N bonds are dehydrogenated via stepwise proton transfer to N then hydride transfer to Fe, whereas relatively nonpolar C–N bonds pass through a concerted proton/hydride transfer transition state.[32] This catalyst was also found to be competent for the reverse hydrogenation of *N*-heterocycles in the presence of a base.[17]

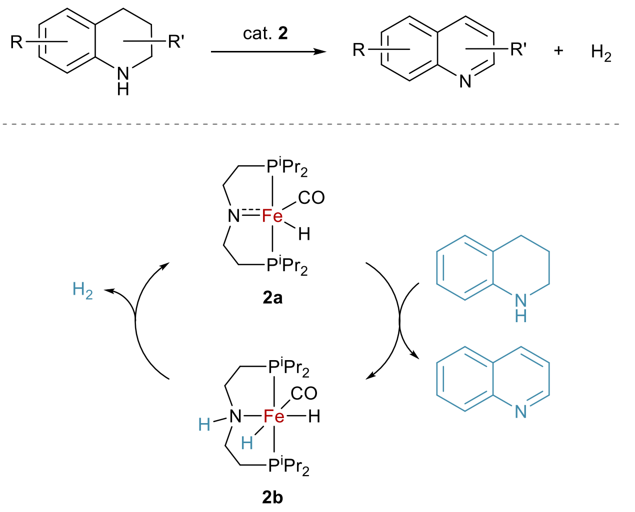

Scheme 3. Proposed mechanism of *N*-heterocycle dehydrogenation catalysed by an Fe(PNP) complex.[17,32]

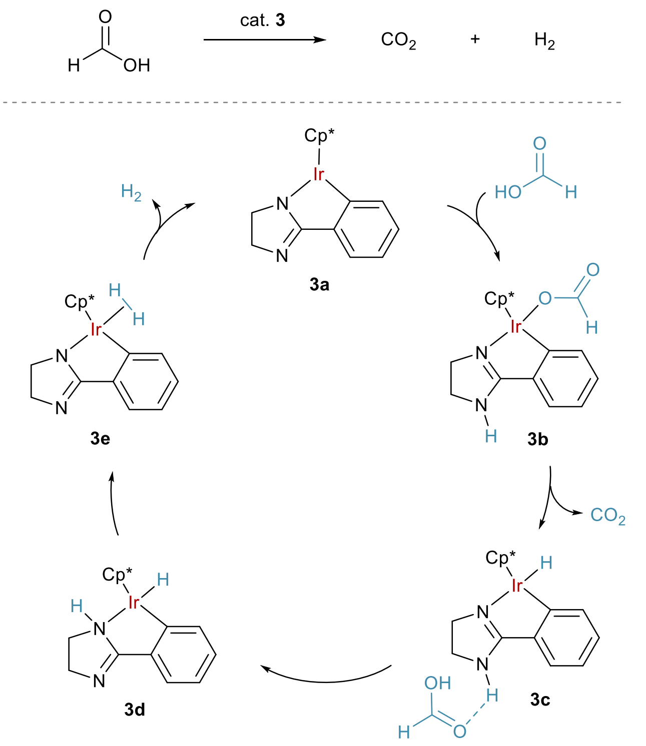

Scheme 4. Proposed mechanism of formic acid dehydrogenation catalysed by an iridium complex featuring a distal Lewis basic amine.[33]

Bifunctional catalysts have also been developed featuring Lewis basic groups remote to the metal site. Xiao and co-workers employed N^C cyclometallated Ir^{III} complexes for the catalytic dehydrogenation of formic acid (Scheme 4).[33] The highest catalytic activity was observed in complexes featuring 2-aryl-imidazoline ligands. The presence of the Ir–N=C–NH unit was found to be crucial to the catalytic performance, with related complexes that did not bear this functionality proving inactive. The proposed mechanism is shown in Scheme 4, where the distal nitrogen acts as a proton shuttle between the formic acid and the proximal nitrogen. Protonation of the distal nitrogen by formic acid generates the formate complex **3b**. Through decarboxylation, the hydride species **3c** is generated, with formic acid hydrogen bonding to the distal NH offering a stabilising effect. This species is proposed to be the catalytic resting state, and can readily be synthesised from the reaction of **3a** with H_2. Proton transfer from the distal nitrogen to the proximal nitrogen ensues, which is proposed to be formic acid assisted, generating **3d**. Intramolecular protonation of the hydride ligand forms a dihydrogen complex **3e**, from which H_2 elimination regenerates **3a**. This type of reactivity is unique in the sense that there are two cooperative Lewis basic sites that participate, and the distal nitrogen is crucial for reactivity.

Carbene complexes can also exhibit metal-ligand cooperativity through reversible bond activation across the M=C bond.[34] Examples of this form of reactivity are rare, however, Gessner and co-workers have reported usage of the ruthenium carbene complex [Ru{C(P(S)Ph_2)(SO_2Ph)}(*p*-cymene)] (**4**) for transfer hydrogenation of ketones using formic acid or ^{i}PrOH as the H_2 source.[18,35] While only moderate yields were achieved, the authors demonstrated catalytic MLC reactivity with these carbene complexes. ^{i}PrOH coordination is the first step of the computed mechanism (Scheme 5). Dehydrogenation proceeds via stepwise deprotonation of the OH group by the carbene and subsequent hydride transfer to Ru to form the resting state **4c**. Hydrogenation of the ketone substrate follows the reverse hydride and proton transfer processes. Both C to Ru and Ru to C hydride transfer steps are calculated to have high energy barriers (>100 kJ mol^{-1}), leading to the modest activities observed.

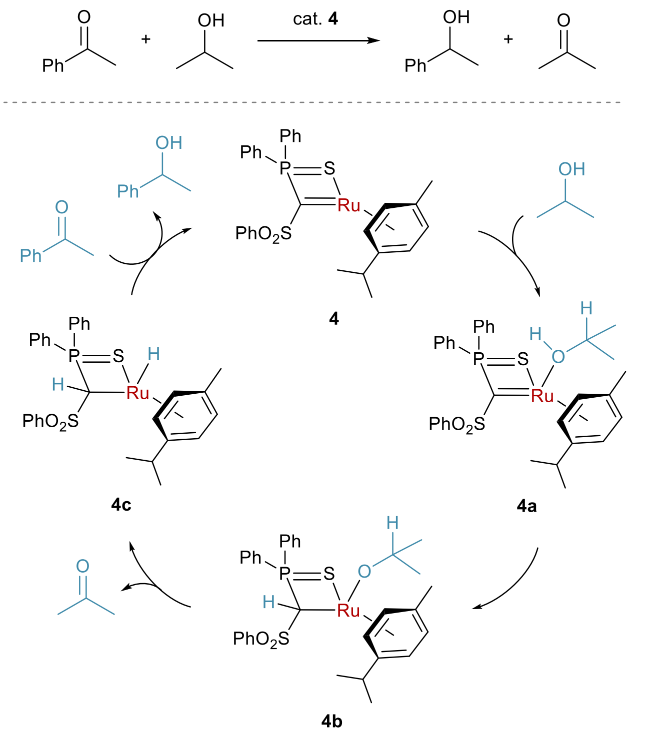

Scheme 5. Proposed mechanism of transfer hydrogenation catalysed by a ruthenium carbene complex.[18,35]

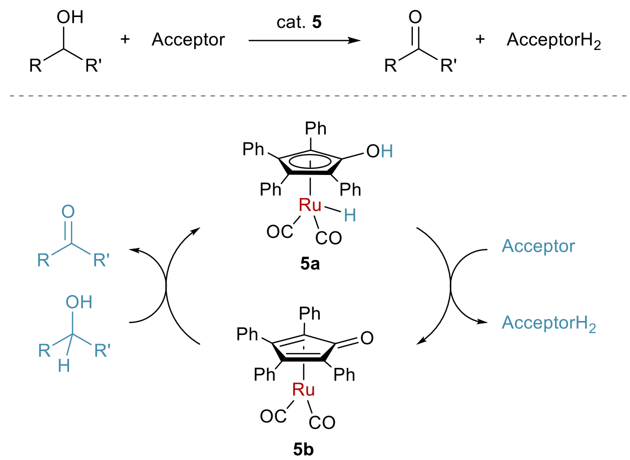

Scheme 6. Proposed mechanism of transfer hydrogenation catalysed by Shvo's catalyst.[36,37]

Aromatisation-Dearomatisation

A highly active area of MLC research encompasses ligands that are capable of undergoing reversible aromatisation-dearomatisation processes. This occurs through proton-responsive Lewis base reactivity, wherein (de)protonation results in a tautomerisation between aromatic and non-aromatic forms of the ligand. A foundational example is Shvo's catalyst, $[Ru_2(\mu\text{-}H)(CO)_4\{(\eta^5\text{-}C_5Ph_4O)_2H\}]$ (**5**), in which the ligand cycles between aromatic hydroxycyclopentadienyl and non-aromatic cyclopentadienone states.[36,37] The catalyst shows high activity in transfer hydrogenation processes. In a typical catalytic cycle, the Ru_2 precatalyst **5** breaks apart into two active species, the Ru^{II} hydride (**5a**) and the coordinatively unsaturated Ru^0 species (**5b**) (Scheme 6). The hydridic species **5a** hydrogenates the substrate through proton transfer from the $\eta^5\text{-}C_5Ph_4OH$ ligand and hydride transfer from the metal centre, resulting in the dearomatisation of the supporting ligand scaffold. This species **5b** is able to perform cooperative alcohol dehydrogenation, where the ketone acts as the Lewis basic proton acceptor, thereby regaining aromaticity. The inclusion of a cyclopentadienone-based ligands appears to be generalisable, and has been extended to numerous other metals, including earth abundant metals such as iron.[38]

One of the most well-known categories are the pyridine-centred pincers pioneered by the Milstein group, who introduced the aromatisation-dearomatisation terminology to describe the reactivity of their [RuHCl(CO)L] systems (L = PNN, PNP).[19] A rigid pincer scaffold offers desirable properties for catalytic applications, including high tunability and stability of metal complexes. In this case, the pyridine pincers feature a non-innocent methylene linker in the *ortho* position, deprotonation of which results in dearomatisation of the ligand (Scheme 7). Cooperative bond activation can occur across the metal-ligand interface in this species, regaining aromaticity in the process. The overall process occurs without any formal change in the oxidation state of the metal. This has enabled extension of catalysis to 3d metals that do not possess easily accessible two-electron oxidation state cycles, particularly Mn and Fe. These PNN and PNP systems have proven so well-suited to N–H and O–H activations that these catalysts have been implemented in a huge range of (de)hydrogenative processes including dehydrogenation of alcohols, dehydrogenative coupling of alcohols or amines and alcohols, and the reverse hydrogenative processes.[39]

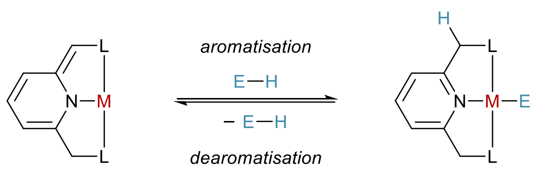

Scheme 7. Reversible aromatisation-dearomatisation processes in pyridine-centred pincer complexes.

In an archetypal example, Milstein and co-workers reported the [RuH(CO)(PNN)] pincer complex **6** for the hydrogenation of amides to amines and alcohols.[40] The conventional proposed mechanism is shown in Scheme 8.[40,41] The reaction is thought to proceed via cooperative addition of H_2 to **6**, resulting in the rearomatised *trans*-dihydride **6a**. Coordination of the incoming amide is facilitated by dissociation of the hemilabile pyridine arm. Migratory insertion of the coordinated amide into the Ru–

H leads to the hemiaminoxy intermediate **6c**. Elimination of the amine is accompanied by dearomatisation, and subsequent addition of H_2 generates the aromatic *trans*-dihydride complex **6e**. Deprotonation of the methylene arm by the alkoxide produces the alcohol and regenerates the initial catalyst **6**.

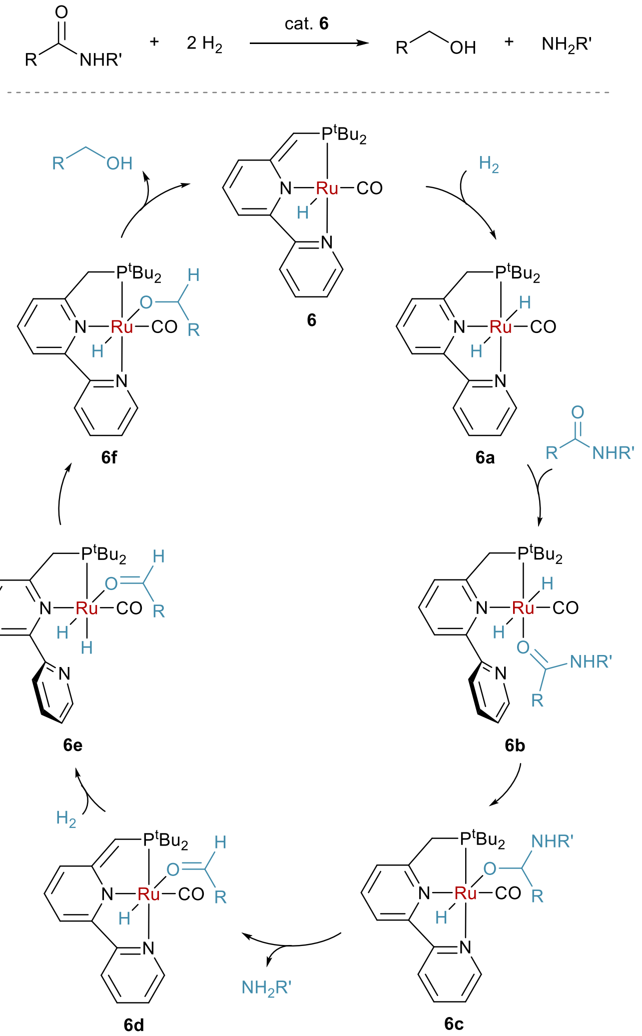

Scheme 8. Proposed mechanism for amide hydrogenation via aromatisation-dearomatisation.[40,41]

Alternative mechanistic pathways have been proposed including single-site (non-cooperative) reactivity via β-hydride elimination.[27] Recent work on PNN systems bearing an NEt_2 side-arm donor has suggested that dehydroalkylation of the CH_2NEt_2 arm can occur during catalytic ester hydrogenation to form a secondary amine donor NHEt.[42] The secondary amine PNN ligand is thought to favour a traditional Lewis base assisted MLC mechanism via protonation-deprotonation of the NHEt moiety, rather than an aromatisation-dearomatisation mechanism.[42] The fact that mechanisms through which prominent catalysts operate are the subject of ongoing debate decades after their discoveries highlights the difficulty in establishing the role of cooperative processes in catalysis.

Metal-Lewis Acid Cooperativity

The other scenario where bifunctional metal-ligand cooperativity is observed is when the ligand acts as a Lewis acid, either directly bound to the metal or as a pendant group, typically through the use of ambiphilic ligands. Reactivity in these MLC systems differs considerably to the other MLC categories and in fact has more similarity with certain MMC catalysts. While (de)hydrogenation reactions by Lewis base-mediated MLC typically involve polar substrates and utilise proton and hydride transfer combinations, Lewis acid MLC catalysts are better known for the hydrogenation of nonpolar alkenes. While H_2 activation has been studied to some extent,[43] reports of catalysis are few, and those in which mechanistic information provides evidence of MLC are extremely limited.

Ligand designs in this category typically feature boron-based Lewis acids. The Peters group have explored the usage of boron-centred pincer ligands as a Lewis acidic moiety. The cobalt complex $[Co(N_2)(PBP)]$ (**7**) is an effective precatalyst for the hydrogenation of terminal alkenes (Scheme 9).[20] Computational studies suggest the dihydride **7a** is the catalytically active intermediate and that the bridging hydride is more reactive than the terminal hydride, illustrating the effect of MLC upon reactivity.[44] Mechanistic modelling by Paul and co-workers[44] found that this species coordinates the incoming alkene, which subsequently undergoes migratory insertion into the bridging Co–H bond. Oxidative addition of H_2 then reductive elimination of ethylbenzene regenerates **7a**. This pincer complex **7** has also been successfully employed in catalytic dehydrogenation of the amine-borane $H_3B{\cdot}NMeH_2$ as well as transfer hydrogenation through combination of the alkene hydrogenation and amine-borane dehydrogenation processes.[20]

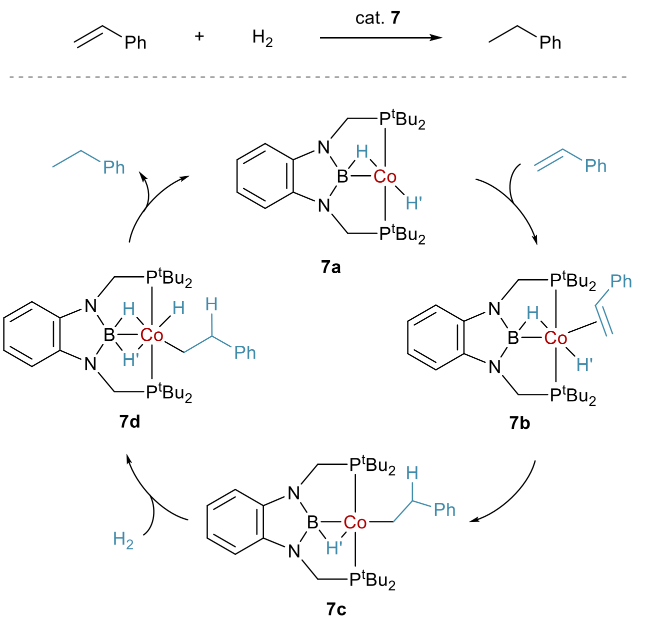

Scheme 9. Proposed mechanism of alkene hydrogenation catalysed by a Co(PBP) complex.[20,44]

In a recent example, Esteruelas and co-workers reported formic acid dehydrogenation catalysed by an Os^{IV} complex **8** with a σ-donating Lewis acidic germylene ligand (Scheme 10).[21] On the basis of experimental rate measurements, Eyring analyses and DFT calculations the mechanism depicted in Scheme 10 was proposed. Dehydrogenation occurs at Os while the decarboxylation proceeds via MLC. The rate law revealed a first order dependence on **8** and a zero order dependence on formic acid. In addition to this, the observation of **8a** as the resting state and calculated barrier heights support CO_2 displacement from Os to form the agostic complex **8b** being rate-determining.

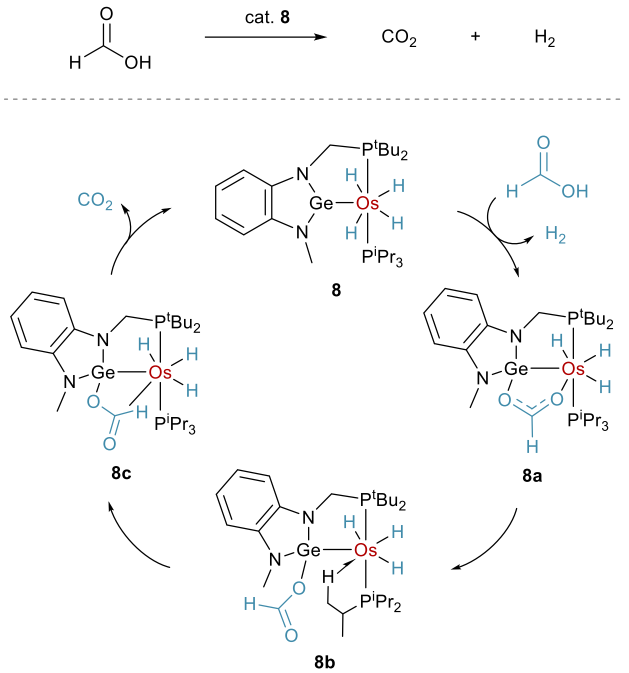

Scheme 10. Proposed mechanism of formic acid dehydrogenation catalysed by an osmium germylene complex.[21]

4. Metal-Metal Cooperativity

In contrast to metal-ligand cooperativity, metal-metal cooperativity in well-defined bimetallic complexes is underdeveloped. Over the past decade much work has been contributed to advance the field such that trends and predictive power are beginning to emerge.[3,5,45] As in MLC, there are a number of ways cooperative reactivity can occur. These can be broadly classified as electronic influences (including redox activity), steric influences, and bifunctional reactivity.[45] In the first two cases substrate reactions occur at one metal centre, with the second metal acting to modify the steric or electronic environment at the active metal site. The focus of this review is on the third category, bifunctional reactivity, in which reversible bond cleavage occurs at both metal centres. It is important to note that the presence of two metals does not necessitate bifunctional reactivity as one of the metals might not be involved, with the reaction proceeding via a monometallic single-site mechanism.[22,23] We have limited the examples included here to those for which there is mechanistic evidence to support both metals playing a functional role in catalysis.

Within the realm of cooperative (de)hydrogenation catalysis, MLC systems are at the forefront, whereas MMC systems are relatively scarce.[6,9,16] This provides an opportunity to compare and contrast these two modes of cooperativity. As seen above, MLC strategies rely heavily on the presence of complementary acidic (e.g. N–H) and hydridic (M–H) moieties. This approach does not directly translate to MMC. Although polarised heterobimetallics can provide Lewis acidic/Lewis basic pairs, in many cases formed M–H moieties would be hydridic in character. Additionally, concerted H_2 oxidative addition or reductive elimination at a metal-metal bond can be symmetry forbidden.[46] However, there are new strategies that are available with MMC. These include participation of metal-metal bonds and bridging coordination modes, the latter of which plays a vital role in almost all the examples covered in this review. As can be seen from these examples, a variety of MMC catalysts exist, ranging from frustrated Lewis pairs and polarised heterobimetallics to nonpolar homobimetallics. Some involve metal-metal multiple bonds or single bonds, but many have no direct metal-metal interaction. A large range of ligand architectures exist, from tethered systems with rigid, highly controlled binding pockets, to flexible tethers, to untethered systems that cycle between bimolecular and unimolecular states throughout the catalytic cycle. Both homo- and heterobimetallic systems feature with similar frequency.

At this stage, (de)hydrogenation involving MMC is limited to sporadic examples which are not easily categorised. There is no universal classification scheme. Sometimes systems are considered based on the degree of metal-metal interaction,[45,47] the ligand scaffold,[45,47] the polarity or Lewis acidity/basicity of the metals,[16] or the mode of substrate activation.[48] Instead, we have presented examples herein by reaction type and substrate.[49] As the field grows, clearer trends and MMC classifications will emerge.

Hydrogenation

Most existing work in MMC hydrogenation is on nonpolar carbon-carbon multiple bonds in alkene hydrogenation and alkyne semihydrogenation reactions, although some examples of CO_2 hydrogenation are known. This differentiates MMC hydrogenation catalysts from MLC hydrogenation and MMC dehydrogenation systems that predominantly catalyse the (de)hydrogenation of polar bonds, with the exception of metal-Lewis acid MLC catalysts. Bridging hydride ligands feature heavily in MMC hydrogenation with both homo- and heterobimetallic catalysts.

Alkyne Semihydrogenation

One of the earliest examples of MMC in catalysis is that of Muetterties and Williams who reported $[Rh_2(\mu\text{-}H)_2\{P(O^iPr)_3\}_4]$ (**9**) for the semihydrogenation of alkynes in 1982 (Scheme 11).[50] This Rh_2 species selectively produces (*E*)-alkenes, in contrast to the generation of (*Z*)-alkenes which occurs with monometallic Rh catalysts. Although the very limited catalyst lifetime (5 min, TOF 1 min^{-1}) restricted synthetic application of this system, its description provided an important early demonstration of how differing mechanistic pathways, reaction outcomes and selectivities can be accessed through MMC.

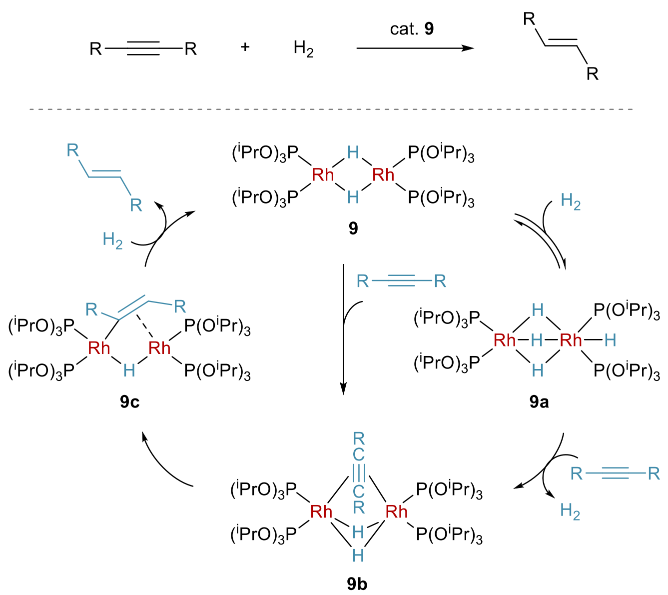

Scheme 11. Proposed mechanism of alkyne semihydrogenation catalysed by $[Rh_2(\mu\text{-}H)_2\{P(O^iPr)_3\}_4]$ (**9**).[50]

The proposed mechanism is outlined in Scheme 11. **9** undergoes fast, reversible addition of H_2. Both species react with alkynes to form a bridging alkyne complex **9b**, which undergoes migratory insertion to form a bridged vinyl **9c**. The *E* stereochemistry of the vinyl species was determined crystallographically. The rate is sensitive to H_2 pressure and the subsequent H_2 addition to **9c** was identified as the rate-determining step (RDS). A key problem in this catalytic system is that reaction of the vinyl intermediate **9c** with alkynes is competitive with the reaction with H_2 to yield product. The outcome of this is degradation of the catalyst within 5 minutes to the insertion product [Rh(π-HRC=CRCR=CR){P(OiPr)$_3$}$_2$], which, as a monorhodium species, displays the conventional selectivity for (*Z*)-alkene production. Catalyst decomposition was supressed by increasing the H_2 pressure from 1 atm to 100 atm, but the accompanying drastic increase in activity led to complete consumption of alkyne within one minute and formation of significant quantities of alkane due to over hydrogenation.

Oro and co-workers have reported mechanistic details of a diiridium alkyne semihydrogenation catalyst $[Ir_2(\mu\text{-}H)(\mu\text{-}Pz)_2H_3(NCMe)(P^iPr_3)_2]$ (**10**, Pz = pyrazolyl, Scheme 12).[51] Catalysis was conducted under mild conditions (rt, 1 atm H_2, 0.2 mol% catalyst), but selectivity was an issue. (*Z*)-stilbene is the predominant product (>90%) at low conversions, but products resulting from slower *Z* to *E* isomerisation and stilbene hydrogenation accumulate at later stages.

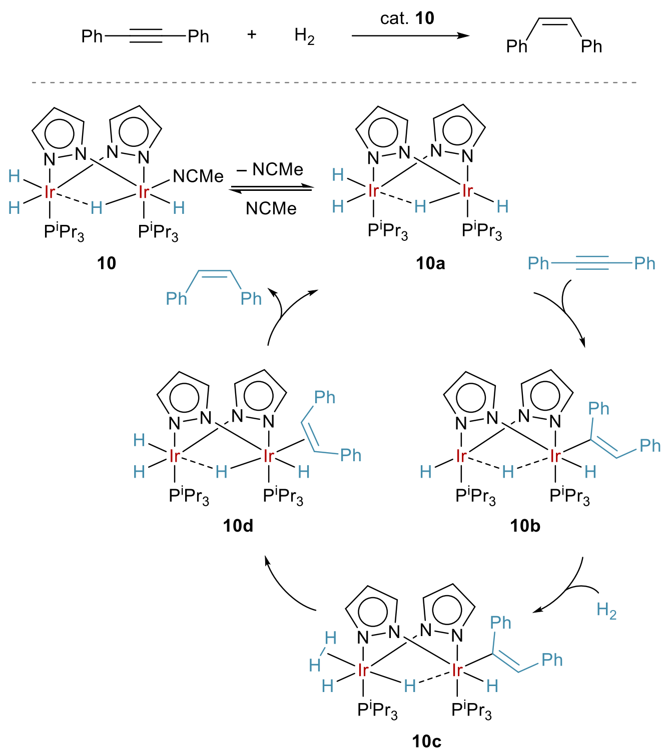

Scheme 12. Proposed mechanism of alkyne semihydrogenation catalysed by diiridium hydride complexes.[51]

Stoichiometric studies allowed identification of several intermediates, both on and off the active catalytic cycle. In the proposed mechanism (Scheme 12), H_2 activation and product elimination occur at different metal centres. This is supported by isotopic labelling studies, wherein treatment of **10b**·NCMe with D_2 yields non-deuterated (*Z*)-stilbene alongside deuterated isotopologues of **10**. Reactivity occurs at the labile sites *trans* to the bridging hydride due to the *trans* effect. While alkyne hydrogenation utilises MMC, the same catalyst in the presence of HBF_4 operates via a monometallic ionic mechanism in the hydrogenation of polar C=N bonds in imine hydrogenation.[23] This example illustrates the role the substrate can play in determining mechanistic pathways.

Mankad and co-workers have developed heterobimetallic systems in which H_2 activation occurs across a M–M′ bond.[52,53] The complexes [Cp(CO)$_2$MM′(NHC)] (**11**, M = Fe, Ru; M′ = Cu, Ag; NHC = *N*-heterocyclic carbene IPr or IMes) are capable of catalysing the semihydrogenation of alkynes with unusual *E* selectivity (Scheme 13). Computations indicated that H_2 cleavage is actually thermodynamically unfavourable with these heterobimetallic systems, confirmed experimentally by the observation of no reaction of [Cp(CO)$_2$MCu(NHC)] with H_2. However, in the presence of an alkyne catalytic conversion is observed at high temperatures and high catalyst loadings (150°C, 24 h, 1 atm H_2, 20 mol% catalyst). [Cp(CO)$_2$RuAg(IMes)] proved to be the most active (96% conversion of diphenylacetylene) and most selective (94% (*E*)-stilbene). Importantly, both metals are required for catalytic activity –

[Ag(OAc)(IPr)] and $[Ru(CO)_2Cp]_2$ exhibited 0% and 7% conversion, respectively.

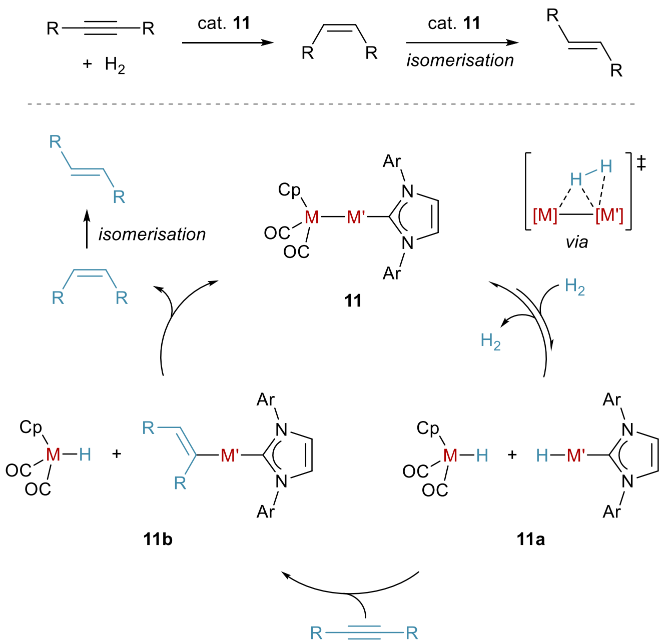

Scheme 13. Proposed mechanism of alkyne semihydrogenation catalysed by group 8-group 10 heterobimetallics (M = Fe, Ru; M′ = Cu, Ag; Ar = Mes, Dipp).[52,53]

The proposed mechanism, shown in Scheme 13, involves cooperative H_2 heterolysis across the M–M′ linkage as the rate-determining step. Detailed DFT analysis of this step reveals that cooperative H_2 cleavage proceeds via an initial H_2 σ-complex at the electrophilic M′ site, accompanied by retrodonation into the H_2 σ* orbital from the nucleophilic M site. The subsequent steps involve *syn*-selective alkyne insertion into the M′–H linkage. Cooperative alkene elimination proceeds via protonolysis of the η^1-alkenyl by the M–H fragment, which liberates the (*Z*)-alkene and reforms the M–M′ bonded species. Subsequent catalytic *Z*-to-*E* isomerisation occurs under the reaction conditions, confirmed by testing the catalytic isomerisation of (*Z*)-stilbene. The authors describe these as d-block analogues of traditional p-block frustrated Lewis pairs (FLPs) because of the complementary nucleophilic (M) and electrophilic (M′) pairing required for the cooperative reactivity observed.

The Thomas group have developed early-late transition metal systems featuring a highly polar Zr≡Co triple bond.[48] The complex $[(THF)IZr\{\mu\text{-}N(Xyl)P^iPr_2\}_2Co(PMePh_2)]$ (**12**, Xyl = 3,5-dimethylphenyl) is an active catalyst for the hydrogenation of terminal alkenes and semihydrogenation of diphenylacetylene thanks to its low activity in hydrogenation of internal alkenes (Scheme 14). The precatalyst **12** features Lewis basic Co^{-I} and Lewis acidic Zr^{IV} sites. Throughout the cycle redox reactivity occurs at Co with Zr playing a stabilising Lewis acid role. The monometallic analogues $[ZrI_2\{N(Xyl)P^iPr_2\}_2]$ and $[CoI(PPh_2NH^iPr)_3]$ displayed no catalytic activity and no H_2 activation ability. High selectivity for alkyne semihydrogenation over alkene hydrogenation is observed (98:2 stilbene:1,2-diphenylethane), but poor *Z*:*E* selectivity (57:43). Both (*E*)- and (*Z*)-stilbene were observed under all conditions tested, even at low conversion time points. As semihydrogenation was much faster than isomerisation, there must be hydrogenation processes that lead to both *E* and *Z* products, although these were not determined experimentally.

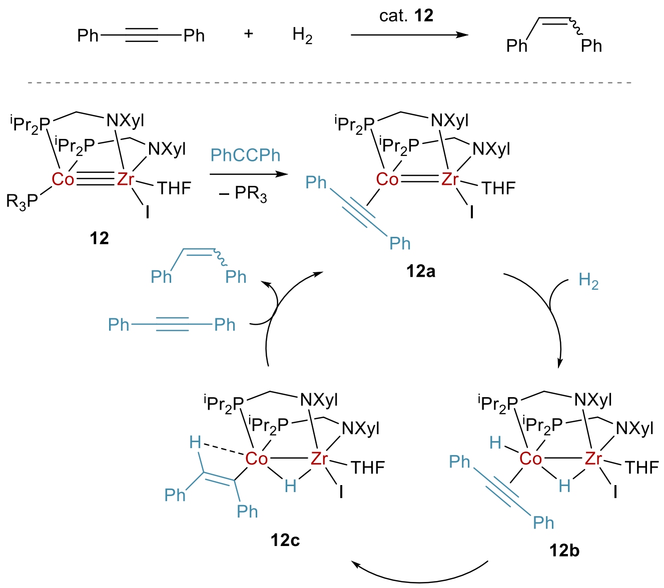

Scheme 14. Proposed mechanism of diphenylacetylene semihydrogenation catalysed by a ZrCo heterobimetallic (Xyl = 3,5-$C_6H_3Me_2$; R_3 = Me_3, $MePh_2$).[54]

A recent computational analysis of the ZrCo system by Ke and co-workers provided a mechanistic proposal (Scheme 14).[54] Displacement of the PR_3 ligand by diphenylacetylene produces the resting state (**12a**) and an entry point to the catalytic cycle. Single-site H_2 cleavage proceeds via oxidative addition at Co. Interaction with the Lewis acidic Zr leads to a more stable bridging hydride (**12b**). Alkyne insertion occurs at the more reactive terminal Co–H, followed by reductive elimination of the alkenyl and bridging hydride ligands. Coordination of diphenylacetylene completes the cycle. The absence of *E*/*Z* selectivity stems from the almost isoenergetic pathways, with the transition state to form the *Z* isomer only 0.1 kcal/mol more favourable (ΔΔG) than that of the *E* isomer. Due to the symmetric disposition of the two P^iPr_2 substituents across the ZrCoCC axis, similar steric interactions occur regardless of which face the α-Ph substituent is disposed towards. The authors show that by modifying the nature of the $XylNPR_2$ R groups, tuning of these ΔΔG values, and thereby *E*/*Z* selectivities, can occur, offering an avenue for the development of selective semihydrogenation catalysts in future.

In another example of polarised heterobimetallics, Lu and co-workers have developed mixed transition metal-main group metal (NiGa) and transition metal-rare earth metal (NiSc, NiY, NiLa, NiLu) systems $[NiM(NPhCH_2P^iPr_2)_3]$ (**13**) capable of *E*-selective semihydrogenation of diphenylacetylene (Scheme 15).[55] All catalysts gave reasonably high conversions (>74%), but differing levels of chemoselectivity and *E*/*Z* stereoselectivity.

Initial rate measurements indicated that NiGa is the fastest for both hydrogenation and subsequent *Z* to *E* isomerisation.

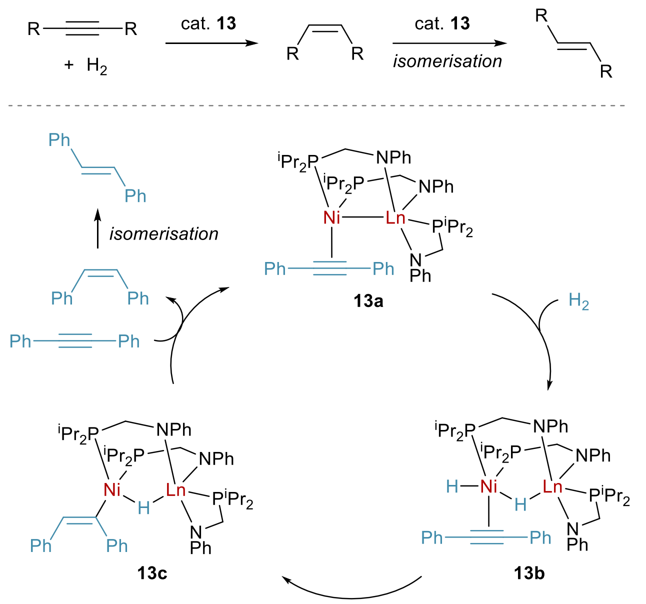

Scheme 15. Proposed mechanism of alkyne semihydrogenation catalysed by $[NiLn(NPhCH_2P^iPr_2)_3]$ complexes (Ln = Lu, Y, La).[55]

The main group and rare earth metals fill the role of a complementary Lewis acidic site to facilitate H_2 activation, while alkyne coordination and migratory insertion both occur at Ni. The constituent steps of the mechanism are the same for all catalysts (alkyne coordination, H_2 oxidative addition, migratory insertion, reductive elimination, e.g. Scheme 15), but the ordering of steps, nature of intermediates, catalyst resting states and relative rates vary depending on the size and Lewis acidity of the M^{III} ion. The strongly Lewis acidic Ga promotes H_2 binding such that the resting state is a Ni(η^2-H_2) adduct. For the larger, less Lewis acidic rare earth metals (Ln = Y, La, Lu), the resting state is the alkyne adduct **13a**.

For **12** and **13**, the mechanisms have some parallels with those seen with MLC catalysts featuring a Lewis acidic site (e.g. **7**, Scheme 9). There is a cross-over MLC-MMC space when considering cooperative systems where the unifying feature is the Lewis acidic behaviour of the cooperative site, regardless of whether it is classified as a metal, metalloid or non-metal. There is value in considering MLC and MMC together in such cases to gain insight from the advances of each.

Alkene Hydrogenation

The only example of asymmetric hydrogenation via MMC has been reported by Reek and co-workers using dirhodium catalysts featuring anionic phosphoramidite-sulfonamido P,N bridging ligands (**14**, Scheme 16).[56] These catalysts were able to hydrogenate hindered acetamidoalkenes with enantioselectivities of up to 99% ee. Kinetic data obtained via gas-uptake measurements provided the rate equation rate = $k[\text{catalyst}][\text{alkene}]^{0.9}[P_{H2}]^{0.5}$. The first order in catalyst is consistent with a bimetallic pathway being operational, whereas if single-site hydrogenation was occurring at each Rh this would be expected to give a rate law that was half order in catalyst. The fractional orders in H_2 and alkene the authors explain computationally by the reversibility of the steps prior to reductive elimination, and the similarity in energies obtained for calculated transition states. **14** was identified as the resting state using high pressure NMR spectroscopy.

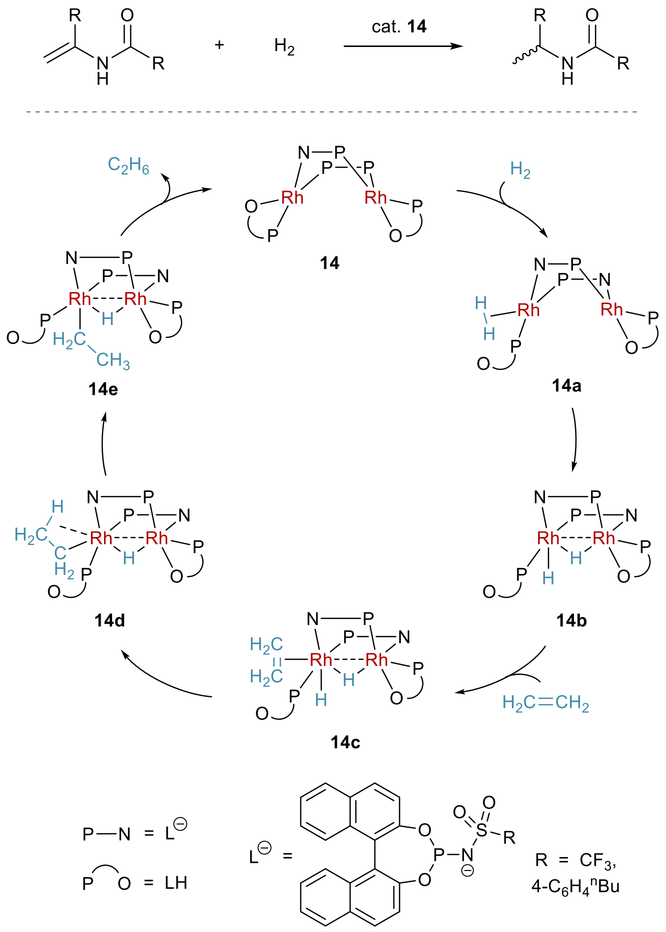

Scheme 16. Proposed mechanism of asymmetric hydrogenation of alkenes by dirhodium phosphoramidite-sulfonamido catalysts.[56]

The mechanism was probed by DFT calculations using a model system for ethylene hydrogenation (Scheme 16). H_2 coordination and ensuing oxidative addition occurs at one Rh centre (forming Rh^{III}), with the second Rh stabilising the formed bridging hydride. Subsequent alkene coordination, migratory insertion and reductive elimination all take place at the Rh^{III} centre. The stabilising role of the second Rh is important as the bridging hydride lowers the energy of the dihydride **14b** by 6 kcal mol^{-1} and ensures a low barrier for H_2 oxidative addition due to cooperative H_2 activation. It is notable that although **14** is homobimetallic, the metal sites become differentiated as Rh^{III} and Rh^{I}, and the mechanism is similar to Lewis acidic MLC and MMC alkyne hydrogenation (**7**, **12**, **13**). This suggests there might be a reasonably universal pathway for cooperative alkene and alkyne hydrogenation. But as the number of examples is still very limited much more work is needed to probe this.

Carbon Dioxide Hydrogenation

The hydrogenative reduction of CO_2 is a topic that has been the subject of considerable research in organometallic catalysis. However, the use of metal-metal cooperative processes is rare, despite being prominent in other methods of CO_2 utilisation such as copolymerisation.[57] Additionally, heterogeneous bimetallic[58] catalysts exhibit high-performance in CO_2 hydrogenation,[59] and homogeneous models could offer mechanistic insight into the cooperative processes.

Llobet and co-workers have found diruthenium polypyridyl complexes to be selective catalysts for the production of formic acid in amine-assisted CO_2 hydrogenation (Scheme 17).[60] In the most active series, the monometallic precatalyst [RuCl(bid)(bpy)] (bid = (*Z*,*Z*)-1,3-bis(pyridin-2-ylmethylene)isoindolin-2-ide) has a faster initial rate (TOF 366 cf 288 h^{-1}), but becomes deactivated after 12 h, whereas the Ru_2 analogue [Ru_2(μ-bpp)(μ-OAc)$(bid)_2$] (bpp = 3,5-bis(2-pyridyl)pyrazolide) retains catalytic activity after 3 days, which is reflected in the 30% increase in TON (1427 cf 1101). The increased stability was proposed to result from the stable bpp-bridged structure avoiding potential decomposition pathways. Kinetic data show the reaction to be first order in catalyst and H_2, but zero order in CO_2.

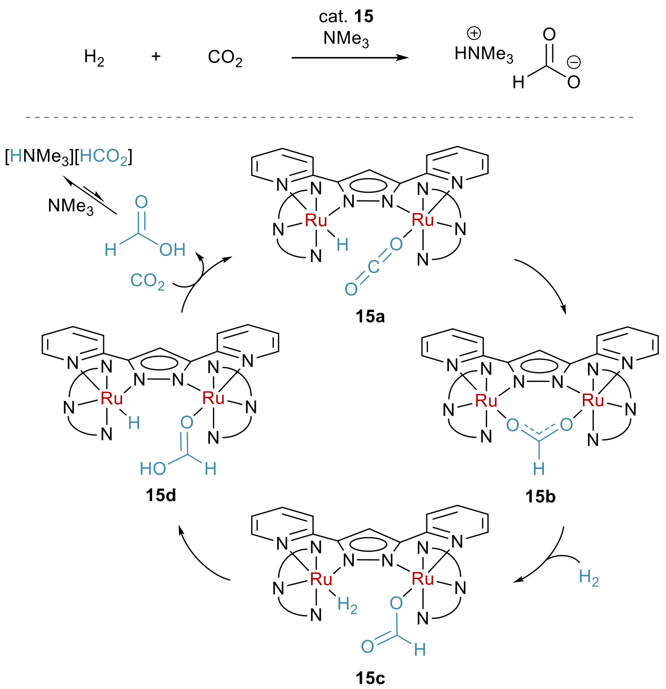

Scheme 17. Proposed mechanism of CO_2 hydrogenation catalysed by diruthenium polypyridyl complexes. Ru(NNN) = Ru(2,2′;6′,2′′-terpyridine)$^+$ (Ru(trpy)$^+$), Ru((*Z*,*Z*)-1,3-bis(pyridin-2-ylmethylene)isoindolin-2-ide) (Ru(bid)).[60]

The calculated mechanism is shown in Scheme 17, in which the active catalyst **15a** is a monohydride with a weakly bound CO_2 ligand. Intramolecular hydride attack generates a bridged formate ligand. MMC effects alter the RDS from formate displacement by H_2 (**15b** → **15c**) in the monometallic systems to heterolytic cleavage of H_2 (**15c** → **15d**) in the bimetallic systems. The heterolytic H_2 cleavage step actually involves MLC with the bound formate as a Lewis basic proton acceptor. The relative ΔG‡ values for the bimetallic systems are lower than the monometallic analogues, in line with experimental findings.

Lau and co-workers found the heterobimetallics [Cp(CO)Ru(μ-dppm)M$(CO)_2$Cp] (**16**; M = Mo, W) were able to catalyse the hydrogenation of CO_2 to formic acid in the presence of NEt_3, albeit with low efficiency (TON ≤ 43; 30 atm CO_2, 30 atm H_2, 120°C, 45 h).[61] The proposed catalytic cycle, outlined in Scheme 18, begins with H_2 activation across the Ru–M bond. CO_2 insertion into the more hydridic Ru–H bond provides the formate anion that is able to deprotonate the bridging hydride of **16c** and reform the metal-metal bonded catalyst. Monitoring the reaction by high pressure NMR spectroscopy revealed that **16** was the only species observed throughout. As such, the low activity was attributed to the non-facile reaction of this catalyst resting state with H_2 to form the dihydride species **16a**. Despite the low TONs, the mononuclear systems [RuCp(CO)(dppm)]$^+$, [RuHCp(CO)(PPh_3)], [RuCp(dppm)Cl]/Ag$^+$, [MCp$(CO)_3$]$^-$ and [MHCp$(CO)_2(PPh_3)$] were all inactive, suggesting that the bimetallic assembly is essential for catalytic activity.

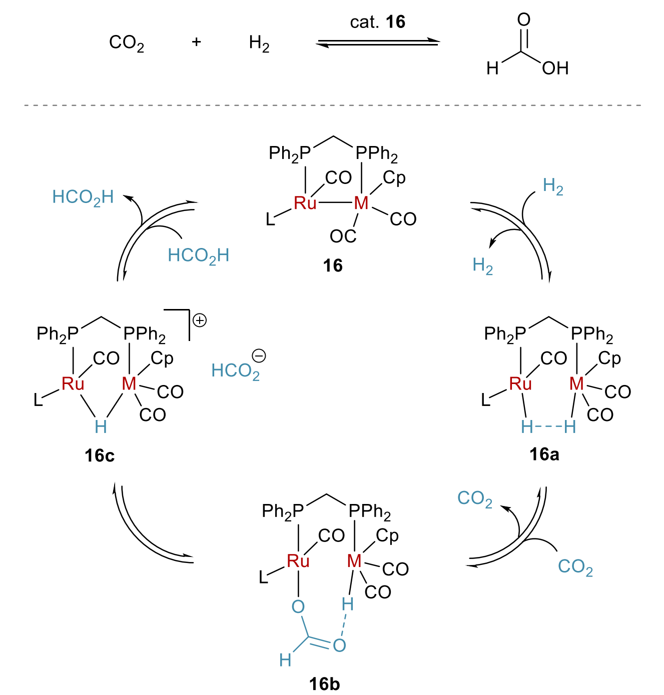

Scheme 18. Proposed mechanism of CO_2 hydrogenation and formic acid dehydrogenation catalysed by RuM (M = Mo, W) heterobimetallics (L = Cp, Cp*).[61]

Puddephatt and co-workers have shown that their formic acid dehydrogenation catalyst [Ru_2(μ-CO)(μ-dppm)$_2(CO)_4$] (**17**, vide infra) is also active for CO_2 hydrogenation in the presence of NEt_3, with a TON ≤ 2160 and TOF ≤ 207 h^{-1}.[62] Data obtained support the mechanism for CO_2 hydrogenation being the reverse of that determined for formic acid dehydrogenation (Scheme 19).

Dehydrogenation

While most of the hydrogenation examples feature nonpolar carbon-carbon bonds, dehydrogenation via MMC is only known for polar substrates, with much of the attention on H_2 generation for energy applications.

Formic Acid Dehydrogenation

The dehydrogenation of formic acid has attracted much attention due to its potential as a hydrogen storage medium, although few bimetallic catalysts are known.[8] An early example of cooperative bimetallic dehydrogenation is the diruthenium precatalyst $[Ru_2(\mu\text{-}CO)(\mu\text{-}dppm)_2(CO)_4]$ (**17**) reported by Puddephatt and co-workers for formic acid dehydrogenation (Scheme 19).[62,63] This catalyst operates at room temperature with low loading (0.6 mol% catalyst, TOF 500 h^{-1}) and high selectivity – only H_2 and CO_2 were detected as products.

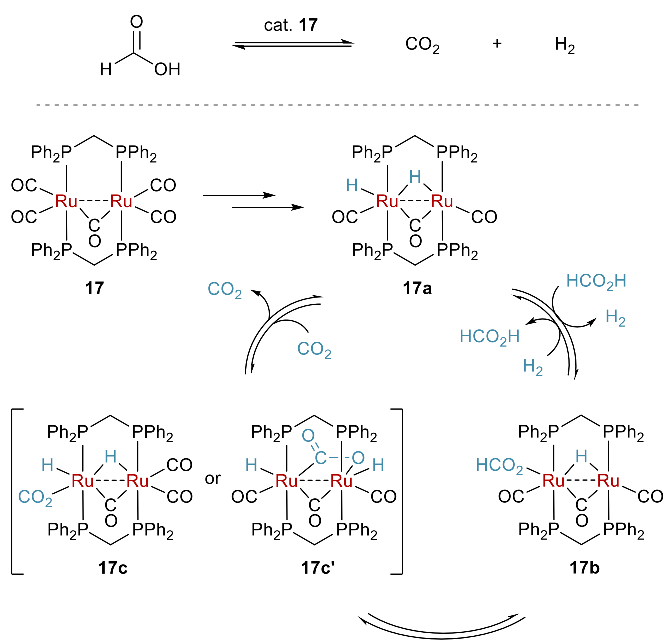

Scheme 19. Proposed mechanism of formic acid dehydrogenation and CO_2 hydrogenation with the $[Ru_2(\mu\text{-}CO)(\mu\text{-}dppm)_2(CO)_4]$ (**17**) precatalyst.[62,63]

The coordinatively unsaturated complex $[Ru_2H(\mu\text{-}H)(\mu\text{-}CO)(\mu\text{-}dppm)_2(CO)_2]$ (**17a**) was identified and postulated to be the active species, with the proposed mechanism outlined in Scheme 19. Kinetic analysis was prevented by the observation of non-linear kinetics, wherein the reaction rate accelerated during catalysis and relative concentrations of Ru species varied. The catalyst resting state is dependent on the pH, and hence on the extent to which formic acid conversion has progressed. Nevertheless, experimental evidence suggests the RDS involves HCO_2^- addition to a Ru_2 complex. Turnover is accelerated by base and supressed by acid or CO, highlighting the importance of pH and vacant coordination sites.

Hong and co-workers have developed $Ir^{III}M^{II}$ systems $[Cp^*ClIr(\mu\text{-}bpp)M(L)(ONO)]$ (**18**; M(L) = Co(H_2O), Ni(MeOH), Cu; bpp = 3,5-bis(2-pyridyl)pyrazolide; ONO = 2,6-pyridinedicarboxylate) capable of aqueous formic acid dehydrogenation in the presence of formate buffer HCO_2H/HCO_2Na (Scheme 20).[64] The heterobimetallic catalysts are up to 350 times faster than their mononuclear analogues, with the IrNi system the best performing (TOF 72 h^{-1}, TON > 4,200). The Ir centre was identified as the site of H_2 evolution, based on the observation of no turnover using monometallic M^{II} analogues $[M(ONO)(H_2O)_n]$ but slow turnover for Ir catalysts $[IrClCp^*(Hbpp)]^+$ or $[IrClCp^*(Mebpp)]^+$. Mixtures of Ir and M monometallic species were much slower than the tethered system, indicating the μ-bpp framework and close proximity of the cooperative metal centres is critical to high catalytic activity. The proposed mechanism (Scheme 20) entails coordination of a bridging formate ligand, followed by bimetallic decarboxylation to yield an Ir–H intermediate **18c**, which was detected spectroscopically, and subsequent protonation to release H_2. Kinetic studies confirmed that the reaction is first order in catalyst, and protonation was proposed as the rate-determining step (**18c** → **18a**).

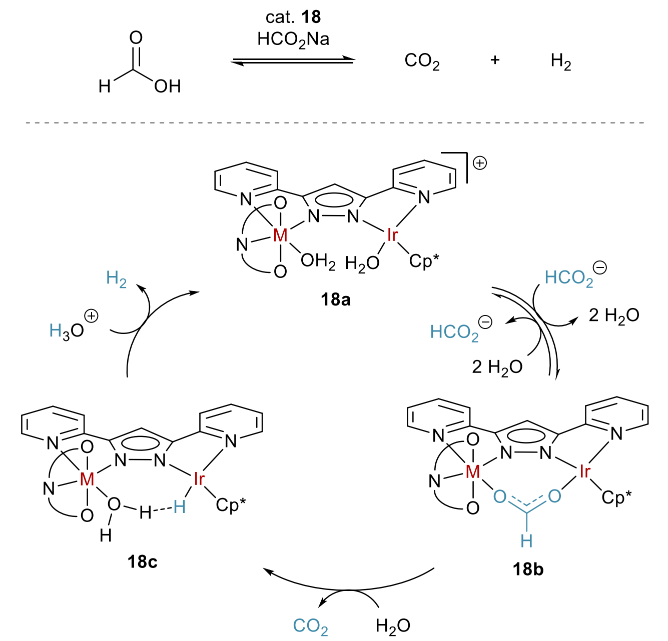

Scheme 20. Proposed mechanism of aqueous formic acid dehydrogenation catalysed by $Ir^{III}M^{II}$ complexes. M = Co, Ni, Cu; ONO = 2,6-pyridinedicarboxylate.[64]

The aforementioned heterobimetallic systems $[L(CO)Ru(\mu\text{-}dppm)M(CO)_2Cp]$ (**16**; M = Mo, W; L = Cp, Cp*), which showed modest activity in CO_2 hydrogenation, were also tested in the reverse reaction formic acid dehydrogenation (Scheme 18).[61] Again modest catalytic activity was observed (complete consumption 6 – 40 h, 80°C, 10 mol% catalyst). NMR monitoring allowed identification of a hydride-bridged intermediate $[Cp(CO)Ru(\mu\text{-}H)(\mu\text{-}dppm)M(CO)_2Cp][HCO_2]$ (**16c**), the detection of which was attributed to the high concentration of formic acid present early in the reaction shifting the equilibrium position. The authors propose that it is the stability of this hydride-bridged intermediate that leads to the low activity. Hydride stabilisation via bridging motifs is a recurrent theme of MMC (de)hydrogenation, but in this example the high stability is detrimental in terms of catalytic activity.

Recent results from Nakajima, Tanase and co-workers provide the first example of effective formic acid dehydrogenation using Cu.[65] The hexameric precatalyst $[Cu_6(\mu_3\text{-}H)_2(Ph_2PCH_2PPh(CH_2)_nPPhCH_2PPh_2)_3(CN^tBu)_4][PF_6]_4$ (**19**, n =1 – 4) was converted into the active unsymmetrical bimetallic species $[Cu_2(\mu\text{-}O_2CH)(Ph_2PCH_2PPh(CH_2)_nPPhCH_2PPh_2)(CN^tBu)_2]^+$ (**19a**) under catalytic conditions. Interestingly, catalytic activity showed a very strong dependence on the nature of the multidentate phosphine ligand (denticity, linker length, stereochemistry), with conversions varying from 0 – 95%. This points to the pivotal role of the spatial relationship between the two cooperative Cu centres. In line with this, the computed mechanism cycles through $Cu_2(\mu\text{-}O_2CH)$ and $Cu_2(\mu\text{-}H)$ complexes (Scheme 21). The absence of hydride species observed during catalysis and a small primary KIE measured using DCO_2H (k_H/k_D 2.98 ± 0.02) point to decarboxylation being the rate-determining step (**19b** → **19c**), which was replicated in the computational study.

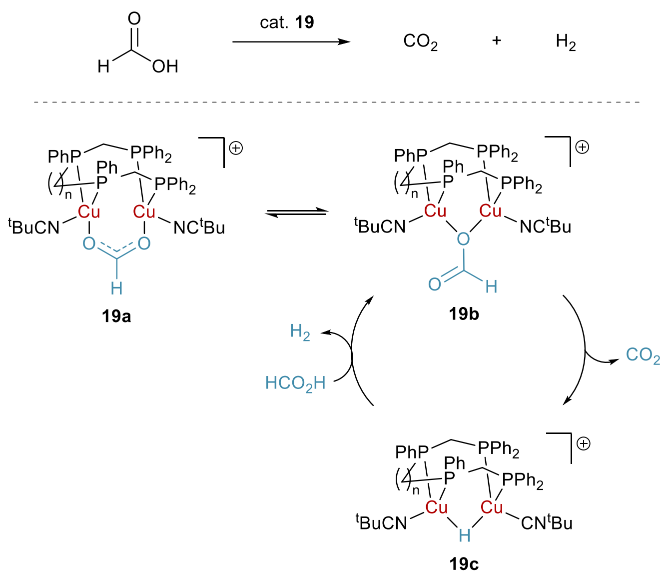

Scheme 21. Proposed mechanism of formic acid dehydrogenation catalysed by dicopper complexes (n = 1 – 4).[65]

Alcohol Dehydrogenation

As seen earlier, MLC strategies have been exceptionally successful in alcohol dehydrogenation. These reactions are widespread due to the utility of the generated carbonyl synthons and transfer hydrogenation reactions as well as applications in hydrogen fuel storage.[9] To date only one MMC example of alcohol dehydrogenation has been reported. Bera and co-workers utilised a metal-metal bonded Ru^{II}_2 2,7-diimine-1,8-naphthyridine construct $[Ru_2(NDI)(OAc)_3]Cl$ (**20**) to catalyse dehydrogenation of a range of alcohols (Scheme 22).[66] Yields of up to 98% were obtained with primary alcohols (70°C, 6 – 24 h, 1 mol% catalyst) with good selectivity for the aldehyde product, but this dropped to ≤48% for secondary alcohols.

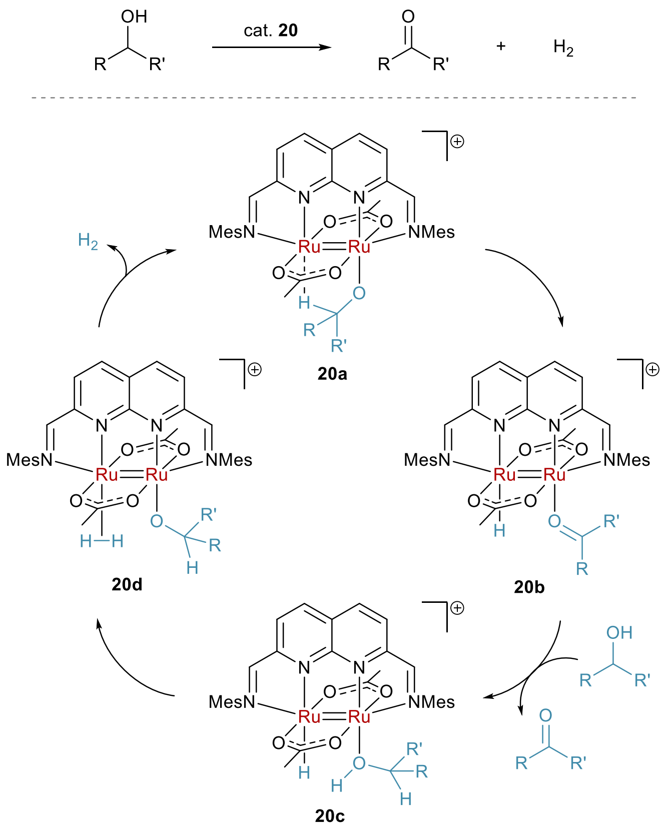

Scheme 22. Proposed mechanism of alcohol dehydrogenation catalysed by a Ru_2 2,7-diimine-1,8-naphthyridine complex.[66]

The proposed mechanism entails reactivity at the Ru sites *trans* to the naphthyridine ligand, with the RuRu bond maintained throughout (Scheme 22). Bimetallic β-H elimination of the bound alkoxide through a 5-membered transition state generates the carbonyl **20b**, which is liberated by an incoming alcohol substrate. Intramolecular proton transfer from the coordinated alcohol **20c** to the bound hydride completes dehydrogenation. Kinetic studies indicated the rate is first order in both catalyst and substrate. On the basis of DFT and KIE studies it was proposed that the final H_2 elimination step is rate-determining. In support of catalysis occurring across the Ru_2 face, the authors show that dehydrogenation of benzyl alcohol using $Ru_2Cl(OAc)_4$, which has an accessible axial site, led to only 30% yield in contrast to 89% yield with the naphthyridine precatalyst **20**, although the differing oxidation states of the precatalysts (Ru_2^{4+} cf Ru_2^{5+}) was not discussed.

Amine-Borane Dehydrogenation

The use of polarised bimetallics provides a promising approach for activating amine-borane substrates, where dehydrogenation requires removal of protic (N–H) and hydridic (B–H) functionalities. Interest in amine-borane dehydrogenation stems primarily from the preparation of inorganic polymers[10] and hydrogen storage materials.[67] Mechanistic studies are typically conducted with the model system $H_3B{\cdot}NHMe_2$ as dehydrogenation produces well-defined molecular products H_2 and $(H_2BNMe_2)_2$ via off-cycle dimerisation of H_2BNMe_2.

Polarised heterobimetallic group 4-group 8 systems [XM(μ-$C_5H_4PEt_2)_2M'Cp^*$] (**21**; M = Zr, Hf; M' = Fe, Ru; X = Me, NMe_2, BH_4) have been investigated in amine-borane dehydrogenation by Nishibayashi and co-workers (Scheme 23).[68] These systems had modest catalytic activities for the dehydrogenation of $H_3B{\cdot}NHMe_2$, $H_3B{\cdot}NH_2Me$ and $H_3B{\cdot}NH_3$, which enabled detailed mechanistic studies of $H_3B{\cdot}NHMe_2$ dehydrogenation (TON ≤ 47, TOF ≤ 9.5 h^{-1}). With the aid of stoichiometric studies using the best performing precatalyst [MeZr(μ-$C_5H_4PEt_2)_2RuCp^*$], a catalytic mechanism was proposed (Scheme 23). N–H activation at Zr precedes B–H activation at Ru. Elimination of H_2 occurs in a cooperative bimetallic fashion forming a Zr–Ru bond. Related monometallic systems such as [MCl_2Cp_2] (M = Zr, Hf)[69] and [$RuHCp^*(Et_2PCH_2CH_2PEt_2)$] were either inactive or much less active. Additionally, the superior performance of the ZrRu system over either HfRu or ZrFe analogues indicates the specialised role each metal plays in catalysis.

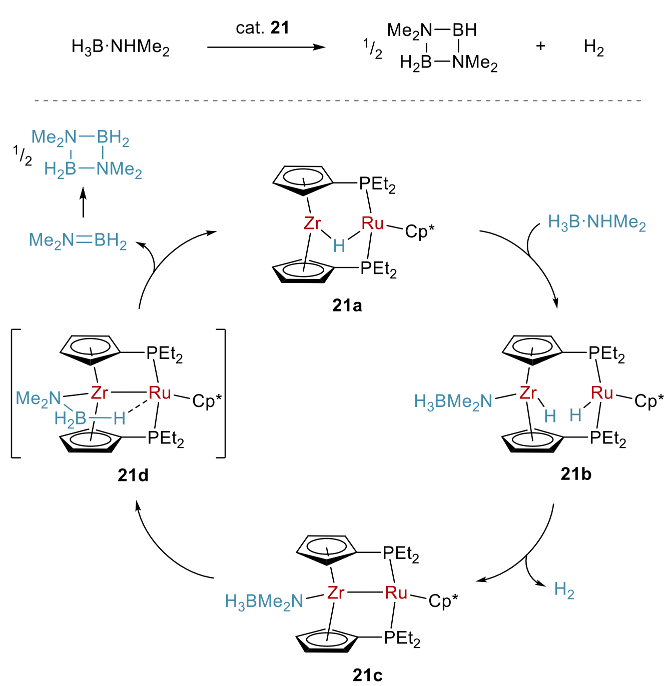

Scheme 23. Proposed mechanism of amine-borane dehydrogenation catalysed by group 4-group 8 heterobimetallics.[68]

Reiß, Beweries and co-workers have investigated a number of dizirconium systems in dehydrogenation of $H_3B{\cdot}NHMe_2$.[22] Detailed experimental and computational studies reveal the most active system [$\{ZrClCp_2\}_2$(μ-$Me_3SiC_3SiMe_3$)]/MeLi operates via a single-site mechanism in which all reactions take place at a single Zr centre. In contrast, the mode of activity of the slower, single-component catalyst [Zr_2(μ-H)(μ-$C_2SiMe_3)Cp_2$] (**22**) does invoke MMC. In the computed mechanism one Zr is responsible for the N–H activation process and the second Zr is the site of B–H activation (Scheme 24). Bimetallic H_2 elimination completes the catalytic cycle. This study illustrates how the presence of two metals is insufficient evidence for MMC, and highlights the need for mechanistic evidence to ascribe cooperative reactivity.

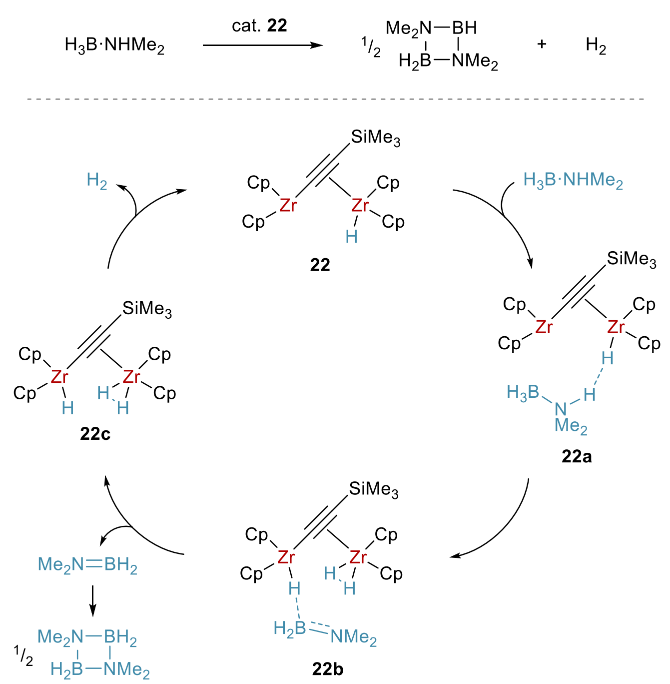

Scheme 24. Proposed mechanism of amine-borane dehydrogenation catalysed by [Zr_2(μ-H)(μ-$C_2SiMe_3)Cp_2$] (**22**).[22]

Another recent example of amine-borane dehydrogenation utilises a bimetallic frustrated Lewis pair system which bears a Lewis acidic Pd site and a Lewis basic W site, reminiscent of MLC strategies (Scheme 25).[70] The two FLP components [Pd(PCP)]$^+$ and [$W(CO)_3L$]$^-$ (L = Cp, Tp) form a bifunctional ion pair (**23**) that can reversibly bind H_2 and dehydrogenate $H_3B{\cdot}NHMe_2$ and $H_3B{\cdot}NH_2{}^tBu$. The individual components [PdH(PCP)], [Pd(PCP)]$^+$, [$WH(CO)_3L$] and [$W(CO)_3L$]$^-$ in isolation showed no activity in dehydrogenation, suggesting the necessity of both metal centres for catalytic activity.

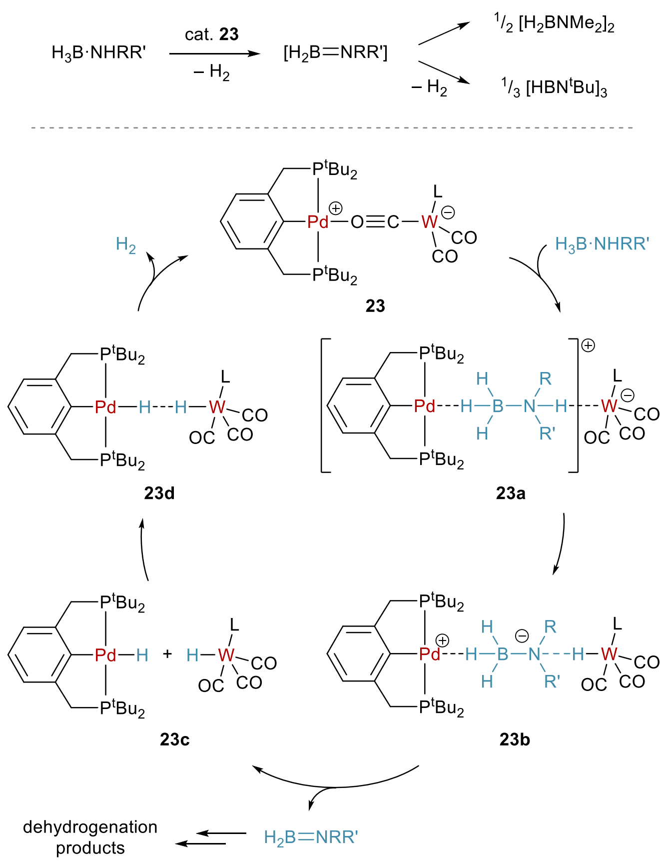

Scheme 25. Proposed mechanism of amine-borane dehydrogenation catalysed by a W-Pd frustrated Lewis pair (L = Cp, Tp).[70]

In the proposed mechanism polarity differences result in association of the amine-borane substrate with a hydridic Pd···HB site and protic W···HN site (Scheme 25). Kinetic data obtained are consistent with a reaction that is first order in catalyst and pseudo-zero order in substrate in the presence of excess $H_3B{\cdot}NHMe_2$. As is commonly the case in amine-borane dehydrogenation,[10] N–H activation is the RDS. The unusually large KIE value (k_H/k_D 20.6 ± 0.3) for $H_3B{\cdot}NHMe_2$/$H_3B{\cdot}NDMe_2$ suggests the likelihood of proton tunnelling. Consistent with proton transfer from coordinated $H_3B{\cdot}NHMe_2$ to $[W(CO)_3L]^-$ being the RDS (**23a** → **23b**), the use of a more basic anion increases the rate of catalysis (L = Tp, k = 0.03 s^{-1}; L = Cp, k = 0.17 s^{-1}). This paper is an important demonstration of the ability of MMC to mimic traditional FLP or MLC reactivity featuring Lewis acidic and Lewis basic sites when designed appropriately.

5. Summary and Outlook

This review has provided a foundational overview of metal-ligand cooperativity in (de)hydrogenation catalysis, and used this insight to examine examples of metal-metal cooperativity. While MLC has a long history and is now a well-established approach in catalysis, MMC is an emerging area that is not yet well understood. Although the diversity of MMC catalyst constructs (e.g. nature of metals, polarity of the metal pairing, degree of interaction, orientation) make it difficult to neatly classify the MMC reactions into categories, there are some clear recurrent features that were highlighted throughout.

Ligands

One of the most universal features in MMC catalysis is the prevalence of bridging ligands, both in active substrate transformation steps and in a more passive stabilising role. Thus an important ligand and catalyst design consideration is the geometric disposition of the two cooperative metal sites in order to facilitate bridging coordination. There is a balance to be found here, as the high stability of the hydride-bridged species **16c** was responsible for its low catalytic activity in CO_2 hydrogenation. Bridging hydrides are encountered in metal-Lewis acid MLC, but typically do not feature in metal-Lewis base or aromatisation-dearomatisation catalysis. Overall, metal-Lewis acid MLC more closely resembles MMC due to the electropositive nature of the Lewis acidic ligand or metal and availability of empty orbitals. Both are relatively underexplored fields, and much can be learnt from considering the two together.

Metal-Metal Complementarity

With the possible exception of the dicopper catalyst **19**,[71] in all the MMC examples covered the two metals perform distinct roles in catalysis, independent of whether substrate transformations involve bridging or terminal coordination. This is similar to MLC systems where the metal and ligand have disparate functions. The diversity of metal pairings indicates that there is no universal combination required for MMC. Homobimetallic and heterobimetallic catalysts feature with similar frequency. The degree of metal-metal interaction spans no interaction to the Zr≡Co triple bond of **13**. Again this correlates with MLC where the cooperative sites can either be directly bonded (typical in metal-Lewis base systems) or remote (e.g. aromatisation-dearomatisation systems). In systems with a direct metal-metal bond, this linkage is often involved in substrate reactivity (as seen in the heterobimetallics **11**, **12**, **13**, **16** and **21**) but not universally so (as seen for the homobimetallic **20**). Reversible cleavage of the metal-ligand bond is less common in MLC, but is known such as in the carbene complex **4** and some metal-Lewis acid systems.

Substrate

The substrate is an important consideration. In metal-metal cooperative (de)hydrogenation of polar substrates, typically substrate binding and reactivity occurs across both metals, as seen here with alcohols, carbon dioxide, formic acid and amine-boranes. In contrast, in hydrogenation reactions of alkenes and alkynes coordination and migratory insertion of the organic substrate tend to occur at one metal, while the second metal facilitates H_2 activation via hydride formation. Substrate specificity is pronounced in MLC reactivity, where metal-Lewis base and aromatisation-dearomatisation processes are the domain of polar substrates, but metal-Lewis acid catalysts are more established for nonpolar substrates. This is related to the mechanisms that are available in each case. As a broad generalisation, with polar substrates the cooperative site acts in a proton-accepting capacity, whereas with nonpolar substrates the cooperative site acts as a hydride-acceptor. Mechanisms for nonpolar substrates rely on the hydride-accepting ability of the cooperative site, which is why both Lewis acids and metals are encountered. A Lewis base is unsuitable for this role due to the lack of an energetically accessible empty orbital, which explains the absence of these catalysts with nonpolar substrates. Conversely, mechanisms for polar substrates rely on the proton-accepting ability of the cooperative site. Hence both Lewis bases and metals can be effective in this role (in practice it is typically a metal hydride rather than the metal that is protonated).

Mechanisms

General mechanisms for metal-Lewis base cooperativity and aromatisation-dearomatisation cooperativity are established, in which hydrogenation of polar substrates proceeds via proton and hydride transfer processes (Figure 2).[1,2,6] However, there is increasing evidence for outer-sphere mechanisms in many of these cases.[24,30]

What has emerged from this review is that a general mechanism exists for alkene and alkyne hydrogenation catalysed by both metal-Lewis acid and MMC systems (Scheme 26), with the exception of $[Rh_2(\mu\text{-}H)_2\{P(O^iPr)_3\}_4]$ (**9**). All transformations involving the alkene/alkyne occur at one metal centre. The cooperative site (metal or Lewis acid) facilitates H_2 activation, typically, but not always, forming a bridging hydride. Hydrogenation proceeds by insertion of the bound alkene/alkyne into the M–H bond followed by reductive elimination of the alkyl/alkenyl ligand and the second hydride, which is delivered either directly from the cooperative site or first transferred to the alkyl/alkenyl-bound metal. There are nuances to this, particularly the order of substrate binding. Nonetheless, this generalised mechanism in which the distinct roles of the cooperative sites is clear will aid understanding and ongoing development of cooperative alkene and alkyne hydrogenation catalysts, and illustrates the importance of a unified examination of MLC and MMC reactivity.

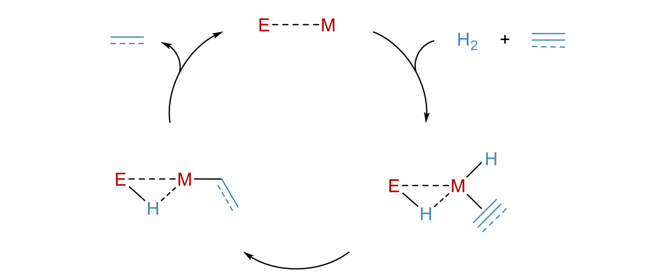

Scheme 26. Generalised mechanism for alkene/alkyne hydrogenation catalysed by metal-Lewis acid (E = Lewis acid) and metal-metal (E = metal) cooperative catalysts.

The mechanisms proposed for (de)hydrogenation of polar substrates by metal-metal or metal-Lewis acid cooperativity are more diverse. As with metal-Lewis base cooperativity, proton and hydride delivery are the key components of the mechanism, but these can occur in a wider variety of ways. In the small number of hydrogenation examples, the mechanism involves substrate insertion into a M–H and protonation by a dihydrogen ligand or bridging hydride. In the case of dehydrogenation, hydride transfer tends to proceed via β–H elimination for formic acid dehydrogenation (decarboxylation) or hydride abstraction for alcohol and amine-borane substrates. The substrate deprotonation step most often involves protonation of a M–H (H_2 formation), but examples are seen where the base is a basic M, a M–M' bond, or external base. This mechanistic diversity reflects the diversity in ligand environments, metal-metal pairings and substrates encountered in MMC catalysis, and showcases the vast potential of the field.

Outlook

The relative maturity of the fields is reflected in the catalytic performance. In most of these isolated examples of MMC (de)hydrogenation, the catalytic activity does not rival that of highly optimised monometallic single-site or MLC catalysts. It does, however, demonstrate interesting breadth of reactivity and modes of substrate activation that will surely be the subject of extensive future developments, ongoing optimisations and more broadly adopted chemical technologies. Both MLC and MMC are evolving fields to watch closely over the coming years.

Cooperative reactivity is being extended beyond binary metal-ligand or metal-metal combinations. Metal-metal-ligand cooperativity (MMLC) from the fusion of bimetallic complexes with non-innocent ligands is an emerging area of research.[72,73] Another interesting scenario is metal-enabled metal-ligand cooperativity, as seen in Bergman's TaIr alkene dehydrogenation catalysts where the Lewis acidity of Ta enables a bound alkyl ligand to act as a hydride shuttle.[74,75] These may emerge as important modes of reactivity in the future design of novel catalysts.

Author Contributions

Both authors contributed to writing and investigation. A L. C. was responsible for conceptualisation.

Conflicts of interest

There are no conflicts to declare.

Acknowledgements

Financial support from the Australian Research Council (A.L.C. Fellowship DE200100450) is gratefully acknowledged.

Notes and references

1 M. R. Elsby and R. T. Baker, *Chem. Soc. Rev.*, 2020, **49**, 8933–8987.

2 T. P. Gonçalves, I. Dutta and K.-W. Huang, *Chem. Commun.*, 2021, **57**, 3070–3082.

3 R. Maity, B. S. Birenheide, F. Breher and B. Sarkar,

ChemCatChem, 2021, **13**, 2337–2370.

4 R. M. Bullock, J. G. Chen, L. Gagliardi, P. J. Chirik, O. K. Farha, et al., *Science*, 2020, **369**, eabc3183.

5 B. Chatterjee, W.-C. Chang, S. Jena and C. Werlé, *ACS Catal.*, 2020, **10**, 14024–14055.

6 J. R. Khusnutdinova and D. Milstein, *Angew. Chem. Int. Ed.*, 2015, **54**, 12236–12273.

7 L. Alig, M. Fritz and S. Schneider, *Chem. Rev.*, 2019, **119**, 2681–2751.

8 K. Sordakis, C. Tang, L. K. Vogt, H. Junge, P. J. Dyson, M. Beller and G. Laurenczy, *Chem. Rev.*, 2018, **118**, 372–433.

9 M. Trincado, J. Bösken and H. Grützmacher, *Coord. Chem. Rev.*, 2021, **443**, 213967.

10 A. L. Colebatch and A. S. Weller, *Chem. – A Eur. J.*, 2019, **25**, 1379–1390.

11 J. Hagen, *Industrial Catalysis: A Practical Approach*, Wiley-VCH, Weinheim, 2015.

12 T. Wall, M. Leist, F. Dietrich, W. R. Thiel and M. Gerhards, *Chempluschem*, 2021, **86**, 622–628.

13 L. Tebben, C. Mück-Lichtenfeld, G. Fernández, S. Grimme and A. Studer, *Chem. – A Eur. J.*, 2017, **23**, 5864–5873.

14 O. R. Luca and R. H. Crabtree, *Chem. Soc. Rev.*, 2013, **42**, 1440–1459.

15 J. M. Blacquiere, *ACS Catal.*, 2021, **11**, 5416–5437.

16 M. K. Karunananda and N. P. Mankad, *ACS Catal.*, 2017, **7**, 6110–6119.

17 S. Chakraborty, W. W. Brennessel and W. D. Jones, *J. Am. Chem. Soc.*, 2014, **136**, 8564–8567.

18 J. Becker, T. Modl and V. H. Gessner, *Chem. Eur. J.*, 2014, **20**, 11295–11299.

19 J. Zhang, G. Leitus, Y. Ben-David and D. Milstein, *J. Am. Chem. Soc.*, 2005, **127**, 10840–10841.

20 T.-P. Lin and J. C. Peters, *J. Am. Chem. Soc.*, 2013, **135**, 15310–15313.

21 M. L. Buil, J. A. Cabeza, M. A. Esteruelas, S. Izquierdo, C. J. Laglera-Gándara, A. I. Nicasio and E. Oñate, *Inorg. Chem.*, 2021, **60**, 16860–16870.

22 K. Lindenau, N. Jannsen, M. Rippke, H. Al Hamwi, C. Selle, H.-J. Drexler, A. Spannenberg, M. Sawall, K. Neymeyr, D. Heller, F. Reiß and T. Beweries, *Catal. Sci. Technol.*, 2021, **11**, 4034–4050.

23 M. Martín, E. Sola, S. Tejero, J. A. López and L. A. Oro, *Chem. Eur. J.*, 2006, **12**, 4057–4068.

24 P. A. Dub and J. C. Gordon, *ACS Catal.*, 2017, 6635–6655.

25 P. A. Dub, N. J. Henson, R. L. Martin and J. C. Gordon, *J. Am. Chem. Soc.*, 2014, **136**, 3505–3521.

26 D. G. Gusev, *ACS Catal.*, 2016, **6**, 6967–6981.

27 D. G. Gusev, *Organometallics*, 2020, **39**, 258–270.

28 M. Yamakawa, H. Ito and R. Noyori, *J. Am. Chem. Soc.*, 2000, **122**, 1466–1478.

29 A. M. R. Hall, D. B. G. Berry, J. N. Crossley, A. Codina, I. Clegg, J. P. Lowe, A. Buchard and U. Hintermair, *ACS Catal.*, 2021, **11**, 13649–13659.

30 P. A. Dub and J. C. Gordon, *Nat. Rev. Chem.*, 2018, **2**, 396–408.

31 P. A. Dub and J. C. Gordon, *Dalton Trans.*, 2016, **45**, 6756–6781.

32 S. M. Bellows, S. Chakraborty, J. B. Gary, W. D. Jones and T. R. Cundari, *Inorg. Chem.*, 2017, **56**, 5519–5524.

33 J. H. Barnard, C. Wang, N. G. Berry and J. Xiao, *Chem. Sci.*, 2013, **4**, 1234–1244.

34 K.-S. S. Feichtner and V. H. Gessner, *Chem. Commun.*, 2018, **54**, 6540–6553.

35 J. Weismann and V. H. Gessner, *Chem. – A Eur. J.*, 2015, **21**, 16103–16112.

36 Y. Shvo, D. Czarkie, Y. Rahamim and D. F. Chodosh, *J. Am. Chem. Soc.*, 1986, **108**, 7400–7402.

37 B. L. Conley, M. K. Pennington-Boggio, E. Boz and T. J. Williams, *Chem. Rev.*, 2010, **110**, 2294–2312.

38 C. P. Casey and H. Guan, *J. Am. Chem. Soc.*, 2007, **129**, 5816–5817.

39 C. Gunanathan and D. Milstein, *Acc. Chem. Res.*, 2011, **44**, 588–602.

40 E. Balaraman, B. Gnanaprakasam, L. J. W. Shimon and D. Milstein, *J. Am. Chem. Soc.*, 2010, **132**, 16756–16758.

41 D. Cantillo, *Eur. J. Inorg. Chem.*, 2011, **2011**, 3008–3013.

42 J. Pham, C. E. Jarczyk, E. F. Reynolds, S. E. Kelly, T. Kim, T. He, J. M. Keith and A. R. Chianese, *Chem. Sci.*, 2021, **12**, 8477–8492.

43 Y. Li, J. Liu, X. Huang, L.-B. Qu, C. Zhao, R. Langer and Z. Ke, *Chem. – A Eur. J.*, 2019, **25**, 13785–13798.

44 G. Ganguly, T. Malakar and A. Paul, *ACS Catal.*, 2015, **5**, 2754–2769.

45 N. Xiong, G. Zhang, X. Sun and R. Zeng, *Chin. J. Chem.*, 2020, **38**, 185–201.

46 G. Trinquier and R. Hoffmann, *Organometallics*, 1984, **3**, 370–380.

47 Q. Wang, S. H. Brooks, T. Liu and N. C. Tomson, *Chem. Commun.*, 2021, **57**, 2839–2853.

48 K. M. Gramigna, D. A. Dickie, B. M. Foxman and C. M. Thomas, *ACS Catal.*, 2019, **9**, 3153–3164.

49 P. Buchwalter, J. Rosé and P. Braunstein, *Chem. Rev.*, 2015, **115**, 28–126.

50 R. R. Burch, E. L. Muetterties, R. G. Teller and J. M. Williams, *J. Am. Chem. Soc.*, 1982, **104**, 4257–4258.

51 F. Torres, E. Sola, A. Elduque, A. P. Martínez, F. J. Lahoz and L. A. Oro, *Chem. Eur. J.*, 2000, **6**, 2120–2128.

52 M. K. Karunananda and N. P. Mankad, *J. Am. Chem. Soc.*, 2015, **137**, 14598–14601.

53 M. K. Karunananda and N. P. Mankad, *Organometallics*, 2017, **36**, 220–227.

54 Y. Li, P. Su, J. Jiang and Z. Ke, *ACS Catal.*, 2021, **11**, 13452–13462.

55 B. L. Ramirez and C. C. Lu, *J. Am. Chem. Soc.*, 2020, **142**, 5396–5407.

56 F. W. Patureau, S. de Boer, M. Kuil, J. Meeuwissen, P.-A. R. Breuil, M. A. Siegler, A. L. Spek, A. J. Sandee, B. de Bruin and J. N. H. Reek, *J. Am. Chem. Soc.*, 2009, **131**, 6683–6685.

57 A. C. Deacy, A. F. R. Kilpatrick, A. Regoutz and C. K. Williams, *Nat. Chem.*, 2020, **12**, 372–380.

58 In this field bimetallic catalysts refer to the inclusion of two different metals. This is in contrast to the use in

homogeneous catalysis in which the term bimetallic describes a molecule containing two metal atoms.
59 M. M.-J. Li and S. C. E. Tsang, *Catal. Sci. Technol.*, 2018, **8**, 3450–3464.
60 T. Ono, N. Planas, P. Mirõ, M. Z. Ertem, E. C. Escudero-Adán, J. Benet-Buchholz, L. Gagliardi, C. J. Cramer and A. Llobet, *ChemCatChem*, 2013, **5**, 3897–3903.
61 M. L. Man, Z. Zhou, S. M. Ng and C. P. Lau, *J. Chem. Soc., Dalton Trans.*, 2003, **3**, 3727–3735.
62 Y. Gao, J. K. Kuncheria, H. A. Jcnkins, R. J. Puddephatt and G. Payap, *J. Chem. Soc., Dalton Trans.*, 2000, **2**, 3212–3217.
63 Y. Gao, J. Kuncheria, G. P. A. Yap, R. J. Puddephatt, P. A. Yap and R. J. Puddephatt, *Chem. Commun.*, 1998, 2365–2366.
64 D. Hong, Y. Shimoyama, Y. Ohgomori, R. Kanega, H. Kotani, T. Ishizuka, Y. Kon, Y. Himeda and T. Kojima, *Inorg. Chem.*, 2020, **59**, 11976–11985.
65 T. Nakajima, Y. Kamiryo, M. Kishimoto, K. Imai, K. Nakamae, Y. Ura and T. Tanase, *J. Am. Chem. Soc.*, 2019, **141**, 8732–8736.
66 I. Dutta, A. Sarbajna, P. Pandey, S. M. W. Rahaman, K. Singh, J. K. Bera, S. M. Wahidur Rahaman, K. Singh, J. K. Bera, S. M. W. Rahaman, K. Singh and J. K. Bera, *Organometallics*, 2016, **35**, 1505–1513.
67 U. B. Demirci, *Int. J. Hydrogen Energy*, 2017, **42**, 9978–10013.
68 T. Miyazaki, Y. Tanabe, M. Yuki, Y. Miyake and Y. Nishibayashi, *Organometallics*, 2011, **30**, 2394–2404.
69 M. E. Sloan, A. Staubitz, T. J. Clark, C. A. Russell, G. C. Lloyd-Jones and I. Manners, *J. Am. Chem. Soc.*, 2010, **132**, 3831–3841.
70 E. S. Osipova, E. S. Gulyaeva, E. I. Gutsul, V. A. Kirkina, A. A. Pavlov, Y. V. Nelyubina, A. Rossin, M. Peruzzini, L. M. Epstein, N. V. Belkova, O. A. Filippov and E. S. Shubina, *Chem. Sci.*, 2021, **12**, 3682–3692.
71 Both μ_2,κ^2-O,H and μ_2,κ^1-H transition states were proposed for hydride abstraction. As such, whether the two metals perform distinct roles in this case is not yet determined.
72 E. Kounalis, M. Lutz and D. L. J. Broere, *Chem. Eur. J.*, 2019, **25**, 13280–13284.
73 M. Li, S. K. Gupta, S. Dechert, S. Demeshko and F. Meyer, *Angew. Chem. Int. Ed.*, 2021, **60**, 14480–14487.
74 M. J. Hostetler, M. D. Butts and R. G. Bergman, *J. Am. Chem. Soc.*, 1993, **115**, 2743–2752.
75 Y. Zhang, S. P. Roberts, R. G. Bergman and D. H. Ess, *ACS Catal.*, 2015, **5**, 1840–1849.